MAY. - AUG. 2022 • Volume XXIII Number

THE ASEAN
JOURNAL OF RADIOLOGY

Highlight

- Original Article
- Case Report
- ASEAN Movement in Radiology

Official Journal of

Radiological Society of Thailand

The Royal College of Radiologists of Thailand,

ASEAN Association of Radiology, and

Foundation for Orphan and Rare Lung Disease

ASEAN
JOURNAL OF RADIOLOGY

ISSN 2672-9393

The ASEAN

Journal of Radiology

CONTENTS

THE ASEAN JOURNAL OF RADIOLOGY
ISSN 2672-9393

From The Editor

The Health of Thai People: COVID-19, monkeypox, dengue fever, and marijuana

Received 28 August 2022 ; accepted 30 August 2022
doi:10.46475/aseanjr.v23i2.184

In spite of having been predicted that there would be a spike in cases and death rates within 1-2 weeks after the Songkran (water splashing) Festival which took place during 13-15 April, the country's Covid-19 situation, instead, has improved and the number of new cases, severe cases and fatalities has declined considerably and continuously to lower than 10, 000 a day since 2 May 2022, compared to the around 20,000 infections daily in the previous weeks. Covid cases were also dropping across ASEAN countries during that period. On 11 May 2022, the first group of fully vaccinated workers from Myanmar were allowed to legally work in Thailand without quarantine. Laos and Thailand agreed to reopen their border check points on 18 May 2022. These good signs initiated the reopening of the nightlife industry which is an important part of tourism in Thailand on 1 June 2022 in 17 provinces and special areas, especially at the tourist islands which can be more easily monitored, referred to as "endemic sandbox" in 14 provinces. The fatalities remained lower than 20 a day and there was no death from COVID-19 reported in Bangkok and southern provinces after 2 weeks of the reopening. It is on 23 June 2022 that the Thai government dropped a mask mandate in all public areas and lift nation-wide COVID-19 restrictions, regardless to the discovery of the COVID-19 Omicron's sub variants BA.4 and BA.5 in more than 180 cases in Bangkok. Wearing a mask is, however, recommended as a voluntary practice in crowded places including on flights. Free treatments at private hospitals, home isolation and community isolation programs for COVID-19 patients ended on 1 July 2022. COVID-19 patients with symptoms receive free treatments at registered hospitals based on their medical benefits and coverage. However, the Thai government maintains the State of Emergency, from 1 August to 30 September 2022, for the need to control the rapid spread of Omicron sub-variants, which was likely less severe but more rapidly spread, especially among children. During the second week of August, the rate of infections was 31, 148 cases a day with 238 deaths, most of whom were people over 60, those with underlying diseases and pregnant women. In the hospital I was working for, during the time of writing this article, around one third of doctors I met had been infected with COVID-19 through their children whose conditions appeared to be much more severe than parents'. Lately, COVID-19 vaccination was advised in children between 3 months to 11 years old to prevent the Multisystem Inflammatory Syndrome in Children (MIS-C) which accounted for more than 100 cases or around 27% of cases in Thailand. The Public Health Ministry accelerated the process of Covid-19 drug registration for general use while the Government Pharmaceutical Organization (GPO) prepared the drugs such as Favipiravir, Molnupiravir and Remdesivir for distribution to the general public for patients doing home isolation, starting on 1 September 2022.

Thailand's first official case of monkey pox in a 27-year-old tourist from Nigeria in Phuket was reported on 21 July 2022 after monkey pox was reported in a transit passenger to Australia a few months before. He visited a hospital because of his skin blisters on 16 July 2022 and the lab tests were confirmed 2 days later when he was subsequently discovered to have departed for Cambodia and was found in Phnom Penh, the capital, on 24 July 2022. On 24 August 2022, the sixth case was reported. Among these 6 cases, 2 were believed to get infected in Thailand. At the time of writing this article, there were around 46,047 cases of monkey pox around the world, more than 70% of which were in America and Europe [1].

Dengue fever, viral infection transmitted to humans through the bite of infected mosquitoes called Aedes aegypti, is an endemic disease throughout the Southeast Asian countries. To draw public concern, every 15th of June is set as ASEAN Dengue Day. Dengue fever outbreaks usually occur about once every two years, increasing cases in this year in Thailand, Vietnam and the Philippines are likely alarming after the decrease in 2020 and 2021. Dengue fever and Covid-19 may share some similar early symptoms such as fever, nausea, vomiting, rashes, and pain. In addition, one patient can have both Covid-19 and dengue fever at the same time, and both diseases can be found in all age groups. The cause of death in patients infected with Dengue virus is internal bleeding. From the beginning of 2022 to 11 July, Thailand reported 9,473 total dengue cases, 7,390 of which were those with dengue fever, 2006 were those with dengue hemorrhagic fever and 77 were those experiencing the dengue shock syndrome including eight deaths. Most deaths from the Dengue infection were likely from Indonesia, the most populated ASEAN country, which comprised of about 228 deaths from January to 5 May 2022 when Thailand reported 3 deaths during that period. Singapore seems to be successful in reducing Dengue fever by cutting mosquito populations by releasing male mosquitoes infected with the Wolbachia bacteria to mate resulting eggs that cannot produce offspring [2]. Dengue fever vaccines are available in some countries with a high dengue fever burden, and is recommended for individuals with a history of dengue infection.

Tourists coming to South East Asia has long been warned of the harsh penalties they face if caught with drug trafficking, even small amounts of marijuana. On 9 June 2022, Thailand has become the first in Asia and the most liberal country to marijuana when she legalised cultivating and consuming cannabis, with the hope that it will bring new sources of income to the farmers, tourist and health care businesses. However, within one week, significant number of consumers reported dizziness and nausea after consuming food and drinks thought to contain cannabis [2]. With the concern of inappropriate use of marijuana in the young, the Ministry of Higher Education, Science, Research and Innovation announced a ban on the sale of food and beverages containing cannabis, as well as the recreational use of cannabis in the universities. On 13 July 2022, after multiple reports of illness and even hospitalization of people after consuming cannabis, the Medical Council of Thailand released 7 guidelines on cannabis and hemp use, stating that only extracts with a known amount of active ingredients could be used in medical purposes only if other medicines are not effective in curing or controlling symptoms of certain diseases. Uses on pregnant and breastfeeding women and those who are under 25 years old, or into food or sweets for the public, or for recreational purposes are not recommended. More than 851 Thai doctors put their names to a letter describing that recreational use of marijuana was a danger to public health in both short and long terms, and called for an immediate end to the liberalization of marijuana.

Wiwatana Tanomkiat, M.D.
Editor,
The ASEAN Journal of Radiology
Email: aseanjournalradiology@gmail.com

References

1. Sanook.com [อินเทอร์เน็ต]. กรุงเทพ: บริษัท เทนเซ็นต์ (ประเทศไทย) จำกัด; 2565 [เข้าถึงเมื่อ 29 สิงหาคม 2565].สธ. ยืนยัน ไทยพบผู้ป่วย "ฝีดาษลิง" รายที่ 6 เป็นหญิงไทย เพิ่งกลับจากกาตาร์. เข้าถึงได้จาก:https://www.sanook.com/news/8614266/

2. ASEAN NOW.com [Internet]. Chonburi: Choice Group Asia Co. Ltd; 2022-06-02 [cited 2022 Aug 29]. Now Dengue fever is spreading across SE Asia. Available from: https://aseannow.com/topic/1261471-now-dengue-fever-is-spreading-across-se-asia/

3. Thaipbsworld.com [Internet]. Bangkok:Thai Public Broadcasting Service; c2018 [cited 2022 Aug 29]. 100+ people treated for symptoms possibly caused by cannabis in food and drink in Khon Kaen. Available from: https://www.thaipbsworld.com/100-people-treated-for-symptoms-possibly-caused-by-cannabis-in-food-and-drink-in-khon-kaen/

THE ASEAN JOURNAL OF RADIOLOGY
ISSN 2672-9393

Original Article

Correlation between shear wave elastography and vibration-controlled transient elastography of liver stiffness in chronic hepatitis B infection in Samut Sakhon Hospital

Yasinee Mekavuthikul, M.D.
Lakkana Jirapong, M.D.
Orawan Autravisittikul, M.D.
From Department of Diagnostic Radiology, Samut Sakhon Hospital, Samut Sakhon, Thailand.
Address correspondence to Y.M. (e-mail: Zippy_niks@hotmail.com)

Received 31 August 2021; revised 12 August 2022; accepted 17 August 2022
doi:10.46475/aseanjr.v23i2.151

Abstract

Background: Assessment of the liver stiffness to evaluate liver fibrosis in viral hepatitis has been an important factor in the management guideline. Due to limitations of liver biopsy, non-invasive assessments of liver stiffness become a more practical method. Vibration-controlled transient elastography (VCTE) has been widely used for a long time and the newcomer, 2D shear wave elastography (2D-SWE) was claimed to possess a strong correlation.

Objective: To assess agreement and correlation of liver stiffness measurement using VCTE and 2D-SWE in patients with viral hepatitis B.

Materials and Methods: 34 patients with a laboratory confirmation as viral hepatitis infected were included. Liver stiffness measurements were obtained using 2D-SWE with VCTE serving as the reference standard on the same occasion. The differences of two measurements were demonstrated by both Bland-Altman and scattered plot. We analyzed their mean differences, 95% limit of agreement, and Spearman correlation (rs) coefficient to determine the agreement and the correlation of the 2D-SWE compared to VCTE.

Results: For VCTE and 2D-SWE, the median elasticity was 5.35 kPa (IQR 4.57, 6.77) and 6.90 kPa (IQR 6.07, 8.25), respectively. The mean differences of the elasticity of tissue between VCTE and SWE were 0.50 kPa (S.D. 3.25 kPa) and 95% limit of agreement was between -6.87 and 5.87 kPa. There was a strong correlation (rs =0.659) between VCTE and 2D-SWE.

Conclusion: In this pilot experience of these two methods, the initial correlation test in real clinical setting has proved a strong measurement correlation between Shear wave elastography and VCTE in hepatitis B patients.

Keywords: 2D shear wave elastography (2D-SWE), Vibration-controlled transient elastography (VCTE), Liver fibrosis.

Introduction

Hepatocellular carcinoma is one of the most common malignant tumors in men and the third most common cancer in women in Thailand [1]. A delay in the diagnosis would lead to poorer prognosis [2]. Therefore, early detection of hepatocellular carcinoma is important for high-risk patients [3]. The most common causes of hepatocellular carcinoma were chronic hepatitis B infection (49.6%), followed by alcoholic cirrhosis (26%), chronic hepatitis C infection (19%), cryptogenic cirrhosis (16%) and non-alcoholic steatohepatitis (2.4%), respectively [1,4-5]. Chronic hepatitis B and C infection caused chronic inflammation and hepatocellular injury with subsequent liver fibrosis and hepatocyte proliferation, promoting liver cirrhosis [4,6-8]. Liver fibrosis, defined as the excessive accumulation of extracellular matrix caused by chronic liver injury, is the key determinant for the prognosis of patients with chronic liver diseases (CLD) [9]. Prior studies suggested that liver stiffness measurement could be a useful predictor of hepatocellular carcinoma development in patient with chronic hepatitis B infection [3]. Because the patients with a mild degree of liver fibrosis or early liver cirrhosis were asymptomatic, the accurate assessment of the degree of liver fibrosis could assist with early diagnosis of liver cirrhosis, prediction of a better disease outcome, and influence on the indication for antiviral therapy [9,10].

Liver biopsy was known to be the gold standard for evaluation in the degree of liver fibrosis [11]. However, this procedure was considered invasive because of its complications. Moreover, equivocal diagnostic accuracy of liver biopsy depended on the sampling specimen [9]. Ideally, a non-invasive method for evaluation of liver fibrosis should be reliable, reproducible, inexpensive, easy to perform, helpful in monitoring disease progression and evaluating treatment efficacy [10]. Recently, liver stiffness measured by noninvasive methods such as transient elastography and 2D-shear wave elastography (2D-SWE) has been reported to be well correlated with liver biopsy [3,9-15]. Following validations in prior cross-sectional studies, transient elastography is now regarded as a reliable surrogate for liver biopsy for grading the severity of liver fibrosis in patients with chronic liver disease [16-18]. 2D-SWE was an excellent modality for evaluating liver fibrosis by itself and provided some strength compared with transient elastography [19, 20]. The aim of this study was to assess the agreement and correlation between 2D-SWE and vibration-controlled transient elastography (VCTE) in patients with hepatitis B virus infection.

Materials and methods

Study subjects

Patients with a laboratory confirmation of HBV infection, in the special outpatient liver clinic of Samut Sakhon Hospital were recruited in the study. Patients were excluded for the following reasons (i) Ongoing CHF (ii) Having focal hepatic lesion (iii) Having ascites (iv) Previous history of hepatic intervention procedure (v) Prior history of antiviral therapy (vi) Performance of 2D-SWE by other radiologists and (vii) Inhomogeneous color map for SWE.

Preparation for vibration-controlled transient elastography (VCTE) and 2D-shear wave elastography (2D- SWE)

All subjects were required to fast at least 6 hours. Patients were placed in supine.

Vibration-controlled transient elastography (VCTE) protocol

Vibration-controlled transient elastography was performed using Fibroscan device (Echosens®) utilizing the medium transducer as per the manufacturer's recommendation. The median value of ten successful acquisitions liver stiffness measurements was calculated and the results were shown in kilopascals (kPa). Grading of liver fibrosis was described below; in Table 1. Because vibration-controlled transient elastography was a valid method to assess liver fibrosis, it was used as the reference method to compare with 2D shear-wave elastography. According to classification stage of liver fibrosis, the cut off values adopted the Metavir score of vibration-controlled transient elastography (Fibroscan) [21].

Table 1. *The interpretation of Vibration-controlled transient elastography parameter in grading liver fibrosis.*

Liver fibrosis	Metavir score	Value (kPa)
No liver fibrosis	F0-F1	1.5-7.0
Non-advance fibrosis	F1-F2	7.1-8.6
Advance liver fibrosis	F2-F3	8.7-10.2
Cirrhosis	F3-F4	10.3-75

2D-shear wave ultrasound shear wave elastography protocol

2D-shear wave elastography was performed by a single radiologist using Toshiba Aplio® 500 and 550 on the same occasion with operator blind to the VCTE results. The radiologist had a 3-year experience in diagnostic radiology and a 2-year experience in ultrasound shear wave elastography and had performed at least 70 cases of ultrasound shear wave elastography before this study. The used probe was a curvilinear probe (5 MHz) via the right hepatic lobe through the intercostal space with the patient lying in a supine position with the right arm in maximal abduction. All patients held their breaths for 5-10 seconds to minimize breathing motion artifacts until obtaining the most adequate window for the liver. The sample box/region of interest (ROI) was located at least 1 cm below the liver capsule and was no more than 5 cm deep from skin with an avoiding area of artifacts and large blood vessel to obtain the best quantitative measurement with a single shot technique. Regions of interest measurements were taken in a circular motion and 1 cm in diameter for 5 times. The median value of five consecutive measurements of all patients was used for statistical analysis and the results were shown in kilopascal (kPa). The median/IQR ratio was less than 0.3 considered to ensure reliable measurement (Figure 1). Grading of liver fibrosis was described below (Table 2) according to the study of Ferraioli et al. [22].

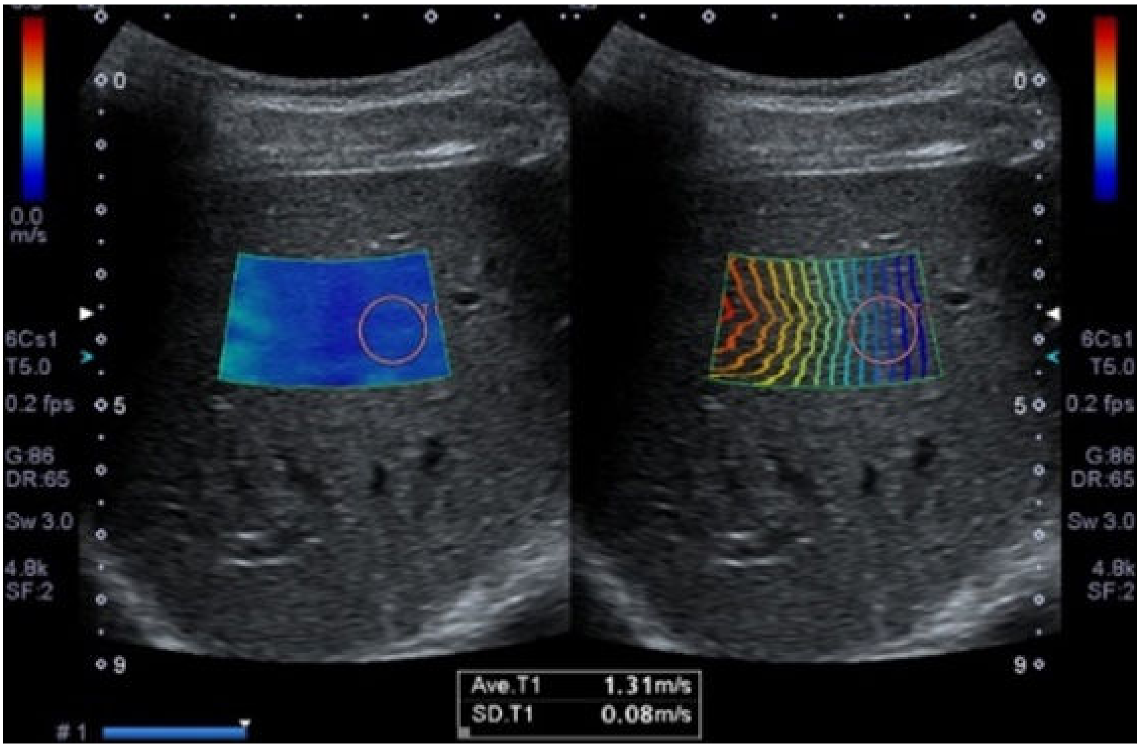

Figure 1. *Speed and propagation maps showing elastogram with 10 mm region of interest.*

Table 2. *Shear wave elastography parameter in grading liver fibrosis [22].*

Liver fibrosis staging	Metavir score	Value (kPa)
No/mild fibrosis	F0-F1	<7.0
significant fibrosis	F2-3	7.0-9.0
severe fibrosis	≥ F3-F4	> 9.0

Statistical analysis

A data analysis was performed using SPSS version 17.0 (IBM Corporation, Chicago, IL, USA). Continuous data were analyzed to assess their normality using the Kolmogorov-Smirnov test and presented as mean and standard deviation or median and interquartile range (IQR) as appropriate. Categorical data were presented as frequency and percentage.

VCTE was used as the reference standard and 2D-SWE was assessed for the differences. Any observed differences between two measurements were analyzed using the Bland-Altman plot, mean difference and its 95% limit of agreement. The correlation between VCTE and 2D-SWE was demonstrated using scattered plot and evaluated for its Spearman's correlation coefficient (rs) using two-tailed significance at p-value of 0.01. Degree of Spearman's correlation coefficient was defined as the followings, 0.00-0.19 "very weak". 0.20-0.39 "weak", 0.40-0.59 "moderate", 0.60-0.79 "strong", and 0.80-1.0 "very strong", respectively.

Ethics consideration

The protocol was approved by the ethic committee of Samut Sakhon Hospital following the ethical guideline of the 1975 declaration of Helsinki and written informed consent was obtained from each patient.

Results

There were 34 patients with a laboratory confirmation of chronic viral hepatitis B infection (by gastroenterologist of Samut Sakhon Hospital), which included immune-tolerant chronic hepatitis B infection (normal or minimally elevated ALT and/or AST levels) or immune-active chronic hepatitis B infection (elevated ALT and/or AST levels), attended in the special outpatient liver clinic of Samut Sakhon Hospital on September 3rd, 2020. The patients were performed noninvasive assessments of liver stiffness using VCTE and 2D- SWE on the same occasion. There was one patient excluded from the study since he was performed 2D-SWE by other radiologists and another one was excluded due to inhomogeneous color map SWE. All in all, there were 32 patients included in this study (Figure 2).

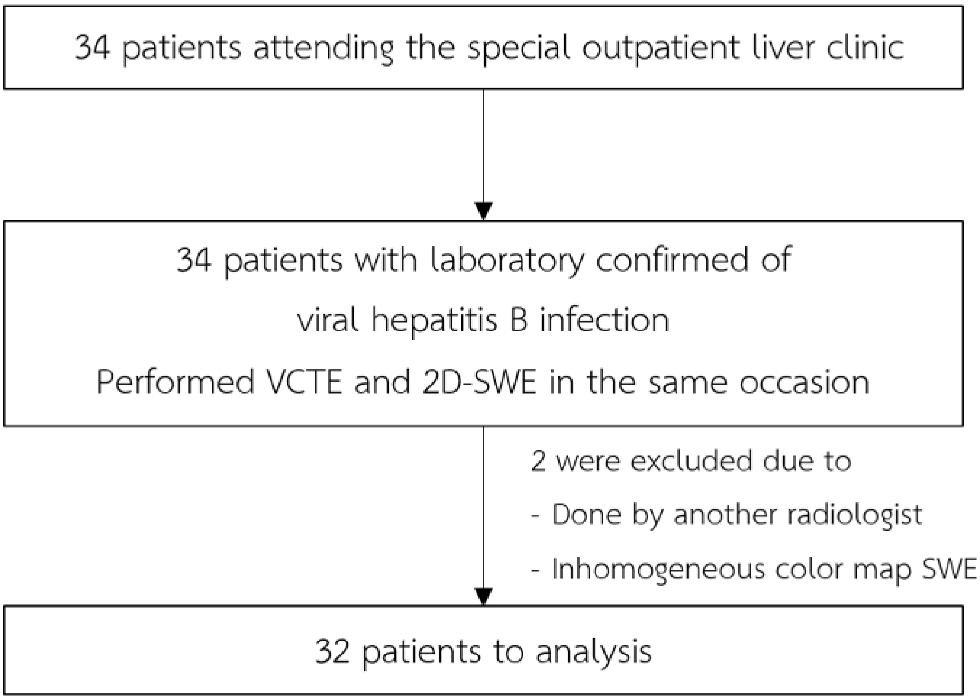

Figure 2. *Flow diagram outlining patient inclusion in this study.*

Among the 32 subjects who were included in the study, there were 10 (31.2%) males and 22 (68.8%) females with the mean age (±standard deviation) of 52.7 years ± 10.5 years. The mean body mass index was 24.5± 3.2 kg/m2. The mean intercostal thickness was 16.7±2.9 mm. The mean AST and ALT were 30±11 IU/L and 30±25 IU/L, respectively (Table 3).

Table 3. *Baseline characteristics of the study subjects.*

Variables	Number (%)	
Sex		
Male	10 (31.2)	
Female	22 (68.8)	
Age (years)		
15-59	23 (71.9)	
≥ 60	9 (28.1)	
Mean (± SD)		52.7 (±10.5)
BMI (kg/m2)		
<25	15 (46.9)	
≥25	12 (37.5)	
No data	5 (15.6)	
Mean (±SD)		24.5 (±3.2)
Intercostal thickness (mm)		
< 25	32(100)	
≥25	0 (0)	
Mean (±SD)		16.9 (±2.9)
AST (IU/L)		
Mean (±SD) IU/L		30 (±11)
ALT (IU/L)		
Mean (±SD) IU/L		30 (±25)

Overall agreement of liver stiffness values between VCTE and 2D-SWE

For VCTE and 2D-SWE, the median elasticity was 5.35 kPa (IQR 4.57, 6.77) and 6.90 kPa (IQR 6.07, 8.25), respectively. The agreement of VCTE and 2D-SWE was elucidated using Bland-Altman plot (Figure 3). The mean differences of the elasticity of tissues between VCTE and 2D-SWE were 0.50 kPa (S.D. 3.25 kPa) and 95% limit of agreement was between -6.87 and 5.87 kPa.

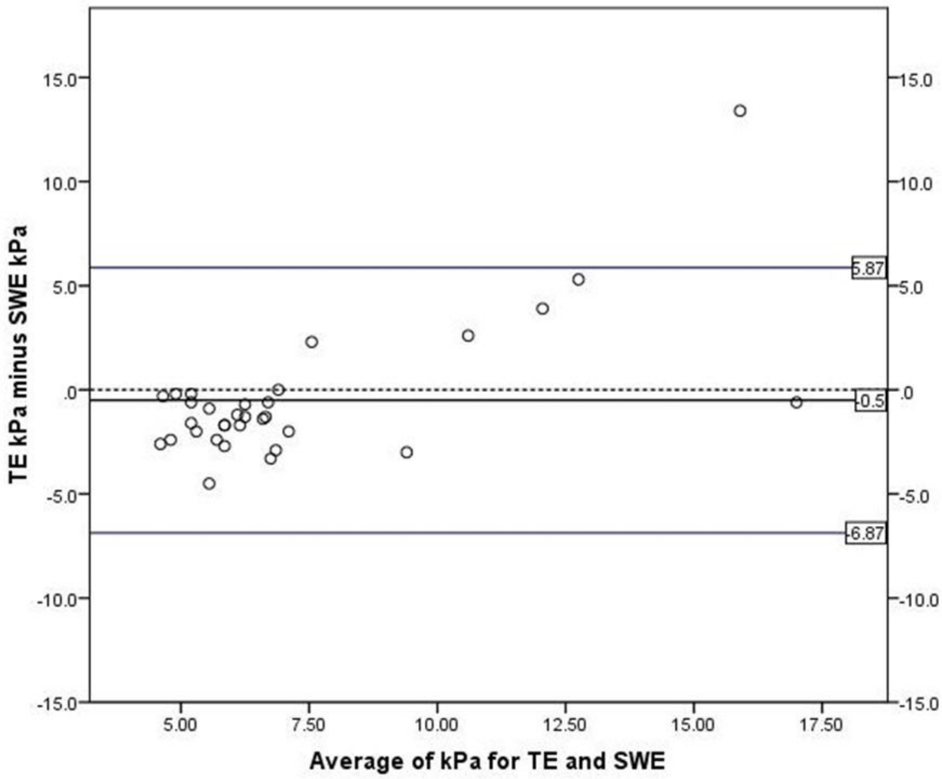

Figure 3. *Bland-Altman plot of VCTE versus 2D-SWE, showing line of mean difference of 0.92 and its 95% limit of agreement.*

The correlation of VCTE and 2D-SWE was demonstrated using scatterplot (Figure 4). Spearman's correlation coefficient was 0.659 (p-value < 0.001), signifying the strong correlation between both tests.

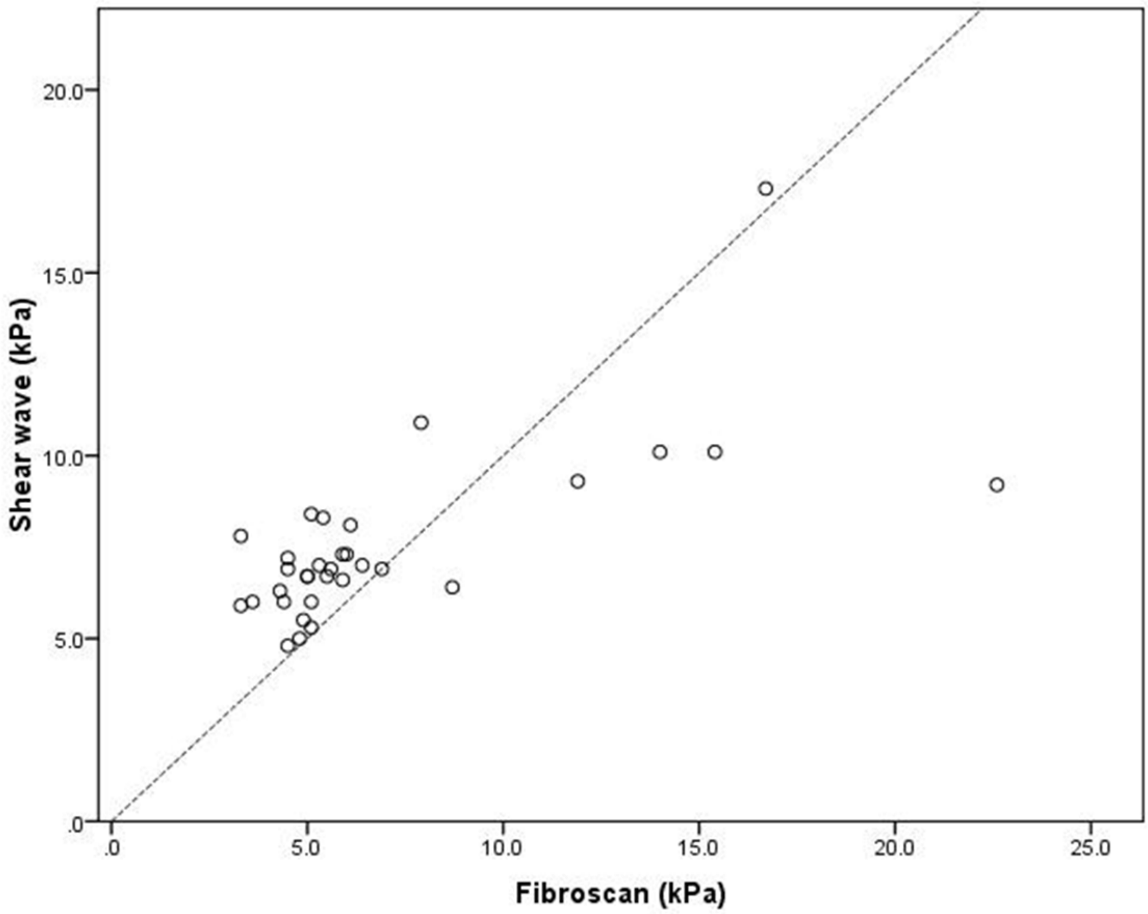

Figure 4. *Scatterplot of transient elastography (VCTE) versus shear wave elastography (SWE) kilopascals demonstrating the line of equal values.*

Discussion

Liver stiffness and fibrosis staging is crucial for treatment of patients with chronic liver disease. In the past, liver biopsy was traditionally used in the indication of fibrosis staging of liver cirrhosis. Nevertheless, the adoption of liver biopsy had its own limitations including sampling errors, bleeding complications and interobserver variations. Instead of liver biopsy, non-invasive measurement (VCTE) has become a more practical technique for assessment of the liver stiffness and fibrosis since 2003 and was considered to be the gold standard non-invasive method. 2D-SWE was a relatively new technique that can be utilized as part of the standard ultrasound examination to asses liver fibrosis. Its agreement and correlation compared to standard VCTE in Thai population were limited for detection of liver fibrosis.

By closely looking into the Bland-Altman plot in our study (Figure 3), we found that the differences between the test tended to be low in the subjects who had low liver stiffness, and the degree of difference tended to be higher as the liver stiffness was higher. This demonstrated the less deviation of liver stiffness (kPa) measured by SWE in no/mild liver fibrosis group (F0-F1, <7 kPa) patients, while in a higher stage of cirrhosis (F2-F4, ≥7.1 kPa), SWE tended to have higher deviation in kPa measured by VCTE. We summarized that SWE had reliable results and helped exclude significant fibrosis.

Our study results revealed that the liver stiffness from 2D-SWE technique achieved a strong correlation (rs =0.659) to the liver stiffness from VCTE technique. Compared to the previous studies, Noola et al [23] and Bende et al [24], who reported strong and very strong correlation (rs=0.66, and 0.83 respectively), our results showed a comparable correlation between the two tests. There were several limitations in this study. One of them is there was a small sample size and most of the recruited subjects were in no fibrosis or an early stage of liver fibrosis groups. Second, when we explored the raw data of the outlier subject, who had liver stiffness of 9.2 kPa and 22.6 kPa, whether measured by SWE or VCTE, respectively, both of the tests graded the patients to the same METAVIR score F3-F4, that did not alter its management on hepatitis B treatment. Third, 2D-SWE is also operator-dependent and our study did not assess the inter-operator and intra-operator variability, which, of course, could to be one of the objectives in the future study.

The advantage of 2D-SWE over vibration-controlled transient elastography (VCTE) is that the 2D-SWE is conducted by radiologists who can use the B-mode ultrasound to evaluate liver parenchyma and real-time choosing the region which is homogeneous parenchyma in the grey scale ultrasound and the color homogeneity in shear wave mode. 2D-SWE can avoid the region of intrahepatic vessels, bile ducts and the liver capsule when the box of region of interest (ROI) is placed. However, there were also limitations of 2D-SWE in patients who had ascites, a thick abdominal wall and could not hold their breaths long enough for the measurement.

Conclusion

In this pilot experience of these two methods, the initial correlation test in the real clinical setting has proved a strong measurement correlation between Shear wave elastography and VCTE in hepatitis B patients.

References

1. Somboon K, Siramolpiwat S, Vilaichone RK. Epidemiology and survival of hepatocellular carcinoma in the central region of Thailand. Asian Pac J Cancer Prev 2014;15:3567-70. doi: 10.7314/apjcp.2014.15.8.3567.

2. Bruix J, Sherman M; Practice Guidelines Committee, American Association for the Study of Liver Diseases. Management of hepatocellular carcinoma. Hepatology 2005;42:1208-36. doi: 10.1002/hep.20933.

3. Jung KS, Kim SU, Ahn SH, Park YN, Kim DY, Park JY, et al. Risk assessment of hepatitis B virus-related hepatocellular carcinoma development using liver stiffness measurement (FibroScan). Hepatology 2011;53:885-94. doi: 10.1002/hep.24121.

4. Chitapanarux T, Phornphutkul K. Risk factors for the development of hepatocellular carcinoma in Thailand. J Clin Transl Hepatol 2015;3:182-8. doi: 10.14218/JCTH.2015.00025.

5. Virani S, Bilheem S, Chansaard W, Chitapanarux I, Daoprasert K, Khuanchana S, et al. National and subnational pPopulation-based incidence of cancer in Thailand: Assessing cancers with the highest burdens. Cancers (Basel) 2017;9:108. doi: 10.3390/cancers9080108.

6. El-Serag HB. Epidemiology of viral hepatitis and hepatocellular carcinoma. Gastroenterology 2012;142:1264-73 e1. doi: 10.1053/j.gastro.2011.12.061.

7. Alqahtani SA, Colombo M. Viral hepatitis as a risk factor for the development of hepatocellular carcinoma. Hepatoma Res [Internet] 2020 [cited 2022 Aug 18];6:58. Available from: http://7b74039fde63b1e554e618a61665d60891d0.pdf

8. Di Bisceglie AM. Hepatitis B and hepatocellular carcinoma. Hepatology 2009;49(5 Suppl):S56-60. doi: 10.1002/hep.22962.

9. Kim JH, Kim MN, Han KH, Kim SU. Clinical application of transient elastography in patients with chronic viral hepatitis receiving antiviral treatment. Liver Int 2015;35:1103-15. doi: 10.1111/liv.12628.

10. Huang R, Jiang N, Yang R, Geng X, Lin J, Xu G, et al. Fibroscan improves the diagnosis sensitivity of liver fibrosis in patients with chronic hepatitis B. Exp Ther Med 2016;11:1673-7. doi: 10.3892/etm.2016.3135.

11. O'Hara S, Hodson S, Hernaman C, Wambeek N, Olynyk J. Concordance of transient elastography and shear wave elastography for measurement of liver stiffness. Sonography [Internet] 2017 [cited 2022 Aug 18];4:141-5. Available from: https://onlinelibrary.wiley.com/doi/epdf/10.1002/sono.12122

12. Castera L, Forns X, Alberti A. Non-invasive evaluation of liver fibrosis using transient elastography. J Hepatol 2008;48:835-47. doi: 10.1016/j.jhep.2008.02.008.

13. Rockey DC, Bissell DM. Noninvasive measures of liver fibrosis. Hepatology 2006;43(2 Suppl 1):S113-20. doi: 10.1002/hep.21046.

14. Castera L, Vergniol J, Foucher J, Le Bail B, Chanteloup E, Haaser M, et al. Prospective comparison of transient elastography, Fibrotest, APRI, and liver biopsy for the assessment of fibrosis in chronic hepatitis C. Gastroenterology 2005;128:343-50. doi: 10.1053/j.gastro.2004.11.018.

15. Masuzaki R, Tateishi R, Yoshida H, Goto E, Sato T, Ohki T, et al. Prospective risk assessment for hepatocellular carcinoma development in patients with chronic hepatitis C by transient elastography. Hepatology 2009;49:1954-61. doi: 10.1002/hep.22870.

16. Ganne-Carrie N, Ziol M, de Ledinghen V, Douvin C, Marcellin P, Castera L, et al. Accuracy of liver stiffness measurement for the diagnosis of cirrhosis in patients with chronic liver diseases. Hepatology 2006;44:1511-7. doi: 10.1002/hep.21420.

17. Foucher J, Chanteloup E, Vergniol J, Castera L, Le Bail B, Adhoute X, et al. Diagnosis of cirrhosis by transient elastography (FibroScan): a prospective study. Gut 2006;55:403-8. doi: 10.1136/gut.2005.069153.

18. Kim DY, Kim SU, Ahn SH, Park JY, Lee JM, Park YN, et al. Usefulness of FibroScan for detection of early compensated liver cirrhosis in chronic hepatitis B. Dig Dis Sci 2009;54:1758-63. doi: 10.1007/s10620-008-0541-2.

19. Wei H, Jiang HY, Li M, Zhang T, Song B. Two-dimensional shear wave elastography for significant liver fibrosis in patients with chronic hepatitis B: A systematic review and meta-analysis. Eur J Radiol 2020;124:108839. doi: 10.1016/j.ejrad.2020.108839.

20. Fu J, Wu B, Wu H, Lin F, Deng W. Accuracy of real-time shear wave elastography in staging hepatic fibrosis: a meta-analysis. BMC Med Imaging 2020;20(1):16. doi: 10.1186/s12880-020-0414-5.

21. Wong VW, Vergniol J, Wong GL, Foucher J, Chan HL, Le Bail B, et al. Diagnosis of fibrosis and cirrhosis using liver stiffness measurement in nonalcoholic fatty liver disease. Hepatology 2010;51:454-62. doi: 10.1002/hep.23312.

22. Ferraioli G, Maiocchi L, Dellafiore C, Tinelli C, Above E, Filice C. Performance and cutoffs for liver fibrosis staging of a two-dimensional shear wave elastography technique. Eur J Gastroenterol Hepatol 2021;33:89-95. doi: 10.1097/MEG.0000000000001702.

23. Noola B, Thongprateep K, Chirapongsatorn S, Saengruang-Orn S. Correlation of liver stiffness in chronic liver disease between fibroscan and 2D shear wave elastography in Phramongkutklao hospital. J Southeast Asian Med Res [Internet] 2019 [cited 2022 Aug 18];3:67-72. Available from: https://www.jseamed.org/index.php/jseamed/article/view/50/45

24. Bende F, Sporea I, Sirli R, Popescu A, Mare R, Miutescu B, et al. Performance of 2D-SWE.GE for predicting different stages of liver fibrosis, using transient elastography as the reference method. Med Ultrason 2017;19:143-9. doi: 10.11152/mu-910.

THE ASEAN JOURNAL OF RADIOLOGY
ISSN 2672-9393

Case Report

Reports of primary and secondary breast lymphoma: Our experience in King Chulalongkorn Memorial Hospital

Sineenart Panichyawat, M.D.[(1)]
Palita Hansakul, M.D.[(2)]
From [(1)] Department of Radiology and Nuclear Medicine, Faculty of Medicine, Burapha University, Chonburi, Thailand.
[(2)] Department of Radiology, Faculty of Medicine, Chulalongkorn University, Bangkok, Thailand.
Address correspondence to S.P. (e-mail: b_am3z@hotmail.com)

Received 14 June 2021 ; revised 19 July 2022 ; accepted 9 August 2022
doi:10.46475/aseanjr.v23i2.135

Abstract

We report four cases of primary breast lymphoma (PBL) and five cases of secondary breast lymphoma (SBL). We illustrate imaging findings in various imaging modalities including mammography, ultrasonography (US), magnetic resonance imaging (MRI) and positron emission tomography (PET) as well as review literature concerning this uncommon condition.

Keywords: Primary breast lymphoma, Secondary breast lymphoma, Mammography, Ultrasonography, Magnetic resonance imaging.

Introduction

Breast lymphoma, malignant neoplasm arising in lymphatic tissue in the breast, is a rare entity affecting the breast. This accounts for only 0.04-0.7% of all malignant breast tumors [1,2] Breast lymphoma can be stratified into primary breast lymphoma (PBL) and secondary breast lymphoma (SBL). PBL is defined as disease involving breast tissue in the absence of prior diagnosis of extramammary lymphoma or evidence of concurrent widespread disease except the ipsilateral axillary lymph node [3]. SBL, diagnosed when the disease is not confined to the criteria of PBL, is slightly more common than PBL accounting for 17% of metastatic disease to the breast. Distinction from breast carcinoma is important because the main modality of treatment is different and unnecessary surgical intervention can be avoided in breast lymphoma.

This review illustrates imaging findings in various imaging modalities of breast lymphoma cases including four PBL cases and five SBL cases in our institution. The radiologists should be aware of these rare entities due to possible differential diagnosis of breast mass.

Primary breast lymphoma

Case 1

A 75-year-old female presented with palpable mass in the left breast for one year. On the physical examination, the patient was found to have a large nontender mass on the left breast and palpable left axillary lymph nodes. She underwent mammography and an US examination demonstrating a large mass at uthe pper mid part of the left breast with a few prominent left axillary lymph nodes (Figure 1 and 2). All the findings were highly suggestive of malignancy and were scored 5 according to the Breast Imaging, Reporting and Data System (BI-RADS). The Core Needle Biopsy (CNB) revealed the diagnosis of diffuse large B cell lymphoma (DLBCL). A further CT scan of the thorax and abdomen and a bone marrow examination showed no evidence of the disease dissemination.

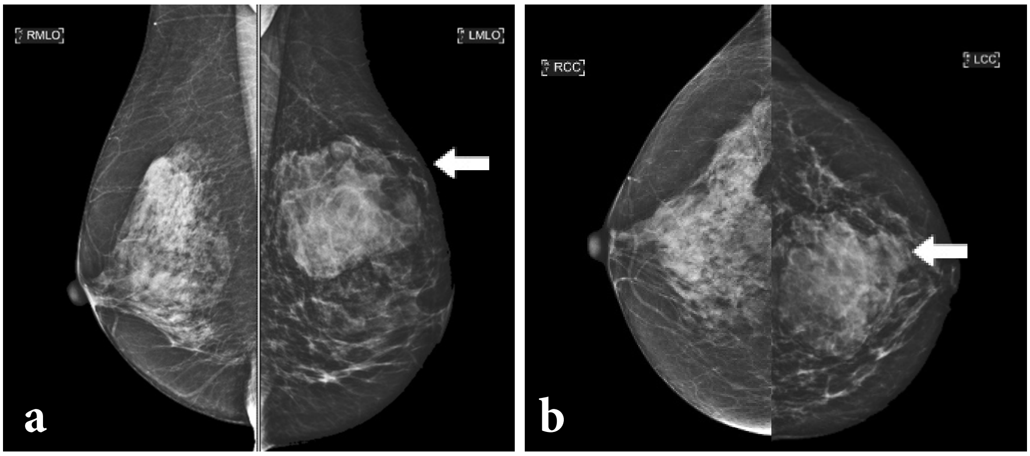

Figure 1. *Mammography (a) MLO (b) CC views show a large oval circumscribed mass with equal density at the upper mid part of the left breast (arrow), measuring about 5.1x3.9x5.7cm.*

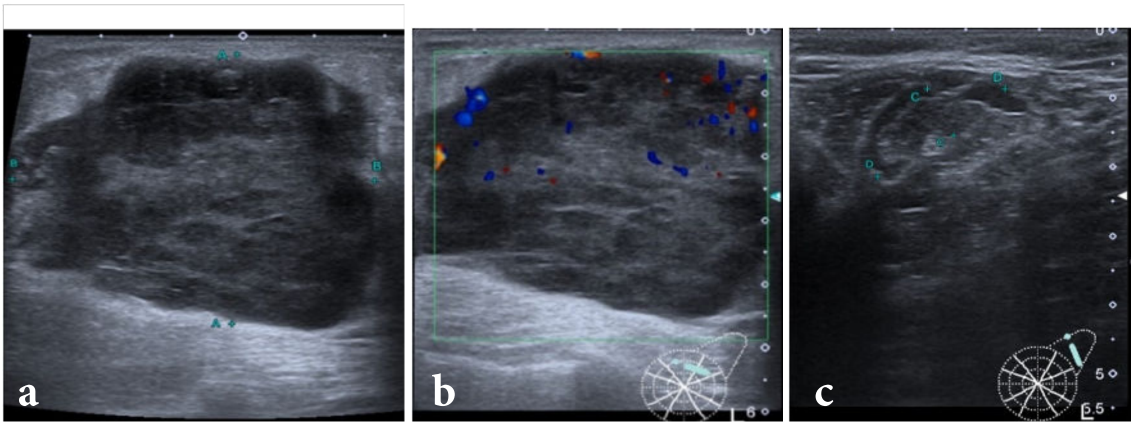

Figure 2. *Ultrasound (a) gray scale (b) color Doppler US of the upper mid part of the left breast reveals a 5.1x4.2x4.7-cm oval circumscribed heterogeneous hypoechoic mass with hypervascularity. (c) US at left axilla shows a left axillary lymph node with eccentric cortical thickening.*

Case 2

A 62-year-old female presented with palpable right axillary mass and right breast lumps for three months. The patient denied of B symptom. The mammography and US confirmed a huge mass occupying nearly the entire right breast and enlarged right axillary lymph node (Figure 3 and 4). She underwent further investigation with breast MRI which revealed two contiguous enhancing masses occupying nearly the entire right breast with multiple enlarged matted right axillary lymph nodes (Figure 5). US-guided CNB showed DLBCL. Staging work-up by CT scan of the chest and the upper abdomen, bone marrow biopsy and CSF examination revealed no other site of disease involvement.

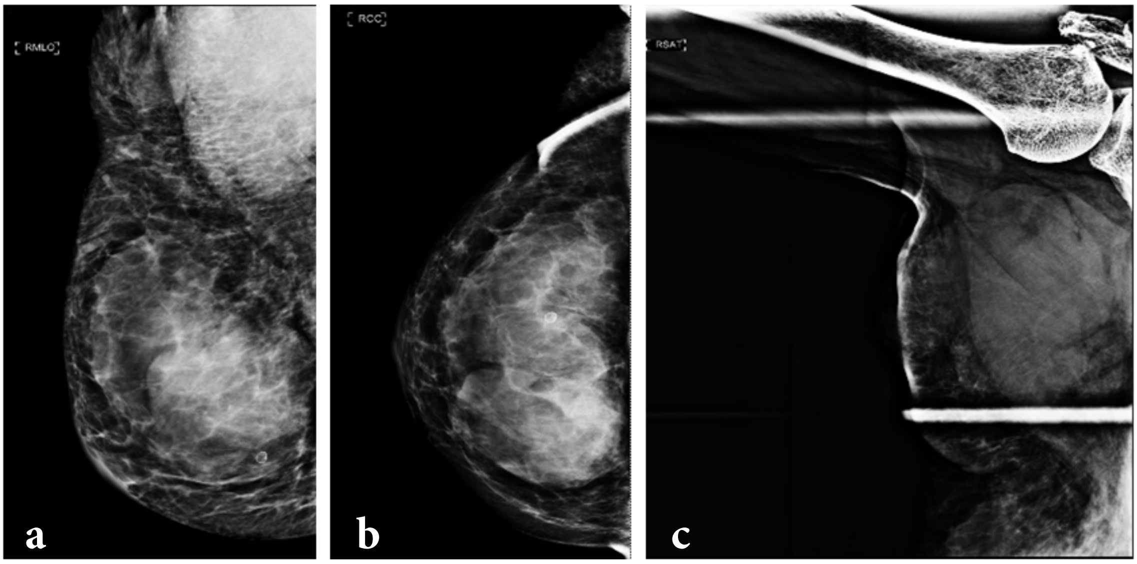

Figure 3. *Mammography (a) MLO (b) CC views of right breast reveal a large oval indistinct hyperdense mass occupying nearly the entire right breast and the (c) right axillary view shows enlarged right axillary lymph node.*

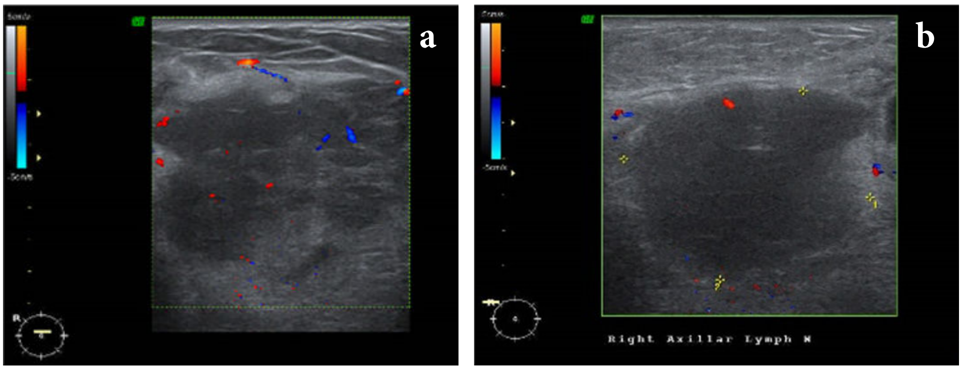

Figure 4. *Ultrasound (a) color Doppler US of the upper part of the right breast and (b) color Doppler US of right axilla shows a large oval indistinct heterogeneous hypo- and hyperechoic mass with increased vascularity at the upper part of the right breast with an enlarged right axillary lymph node with the loss of fatty hilum.*

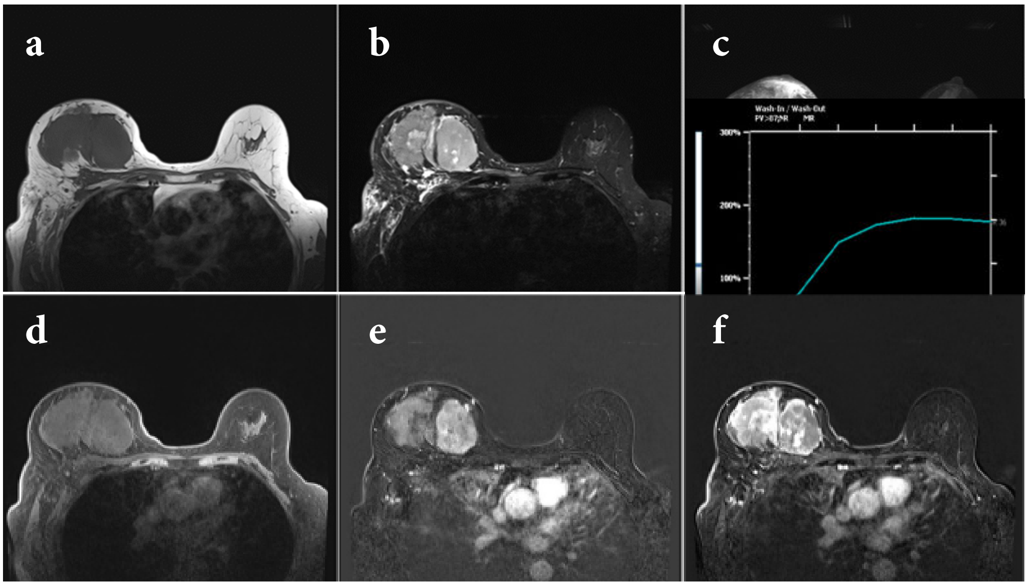

Figure 5. *Breast MRI (a) T1-weighted axial image (b) T2-weighted IR axial image (c) Kinetic curve assessment (d) Fat-suppressed precontrast T1-weighted axial image (e) Fat-suppressed post contrast T1-weighted axial image with subtraction (early phase) (f) Fat-suppressed post contrast T1-weighted axial image with subtraction (delayed phase).*

MRI shows two contiguous oval circumscribed enhancing masses occupying nearly the entire right breast, about 4.3x5.0x5.7 cm and 4.0x4.6x6.1 cm. These masses show heterogeneous iso-to slight hypointensity on T1-weighted image, hyperintensity on T2-weighted image, strongly heterogeneous enhancement with type II kinetic curve and restricted diffusion (ADC= $0.165\text{-}0.623 \times 10^{-3} mm^2/sec$).

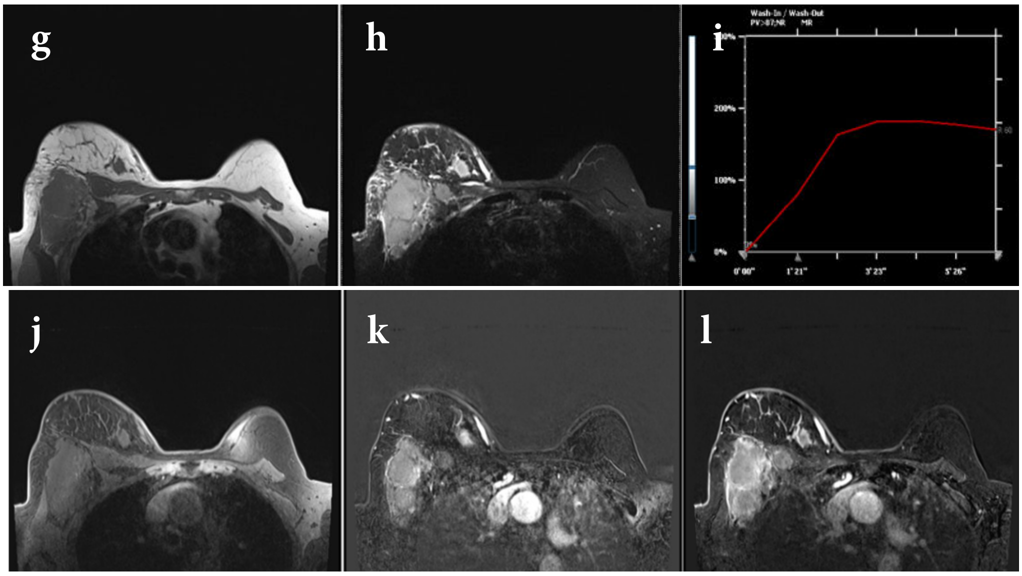

Figure 5. *(continued) Breast MRI (g) T1-weighted axial image h. T2-weighted IR axial image (i) Kinetic curve assessment (j) Fat-suppressed precontrast T1-weighted axial image (k) Fat-suppressed post contrast T1-weighted axial image with subtraction (early phase) (l) Fat-suppressed post contrast T1-weighted axial image with subtraction (delayed phase).*

There are conglomerated enhancing masses with similar signal intensity to the breast masses in the right axilla, totally measuring about 8.3 x 7.2 x 11.8 cm, likely matted lymph nodes.

PET-CT after completion of chemotherapy demonstrated complete metabolic remission (Figure 6).

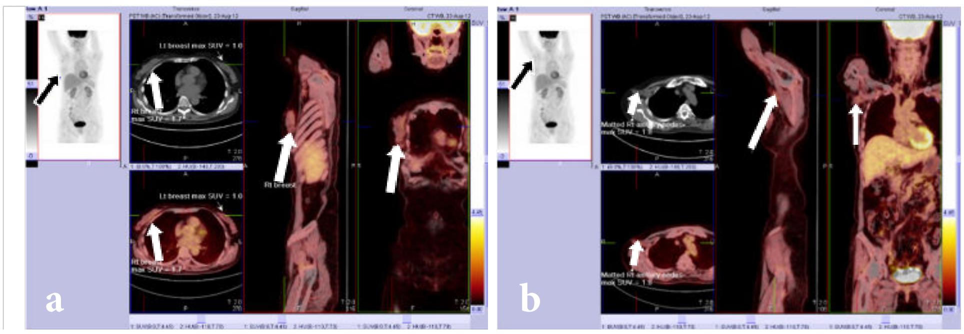

Figure 6. *PET-CT after completion of chemotherapy (a) the right breast (b) the right axilla demonstrates mild thickening of the fibroglandular tissue of the right breast without definable mass and mild soft tissue thickening at right axillary region with non-significant FDG avidity (arrows), radiologically favorable complete response.*

Case 3

A 43-year-old female had a rapidly growing right breast mass for two months. The patient denied of B symptom.

The mammography revealed enlargement of the right breast with global asymmetry (Figure 7. US showed a few irregular indistinct hypoechoic lesions with hypervascularity along the outer part of the right breast (Figure 8). No other evidence of metastatic disease was seen on other staging workup. The incisional biopsy of the breast mass confirmed diagnosis of DLBCL.

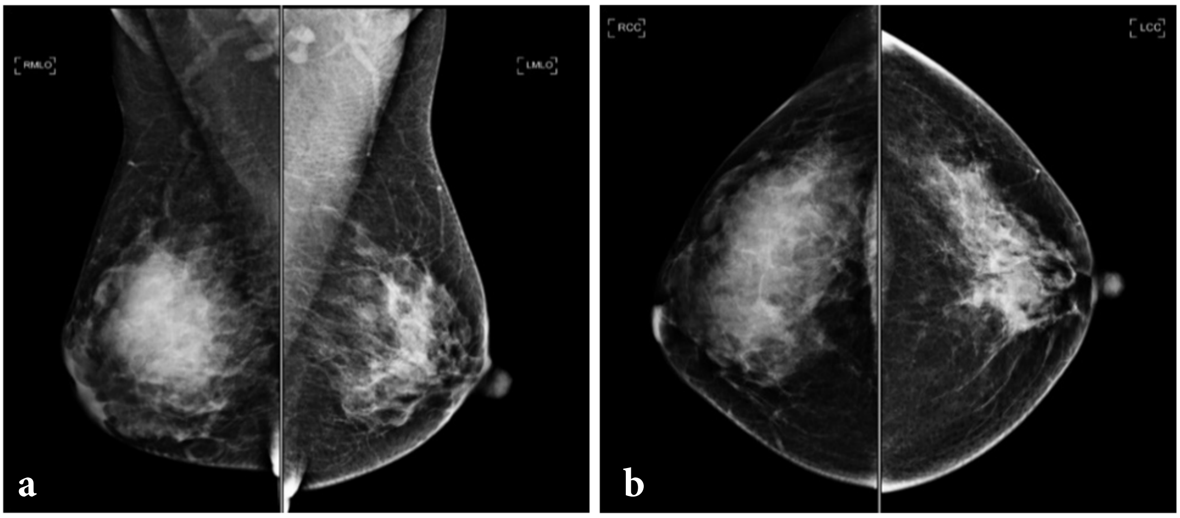

Figure 7. *Mammography (a) MLO (b) CC views reveals enlargement of right breast with global asymmetry.*

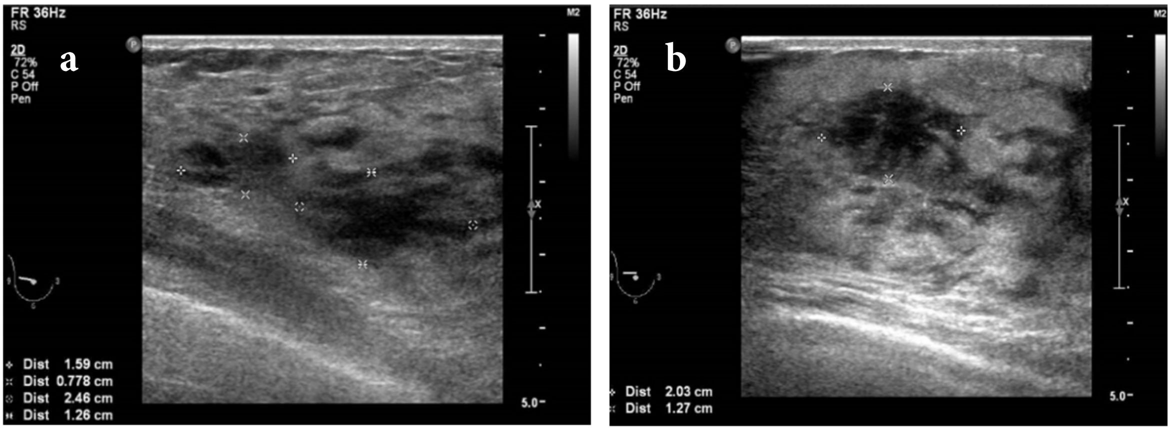

Figure 8. *Ultrasound (a) and (b) gray scale US of the upper outer part of the right breast shows a few irregular indistinct hypoechoic lesions along the outer part and the central region of the right breast, measuring up to 2.5x1.3 cm. Increased echogenicity of overlying subcutaneous fat is also noted.*

Case 4

A 30-year-old female presented with palpable mass on the right breast for four months. Initial US demonstrated a circumscribed mass at the upper mid part of the right breast (Figure 9). The mammography and US performed two months after the initial study revealed a much increased size of the mass n the right breast (Figure 10 and 11). US-guided CNB of the breast mass comfirmed diagnosis of DLBCL. CT scan of the chest and the whole abdomen and bone marrow biopsy revealed no other site of disease involvement.

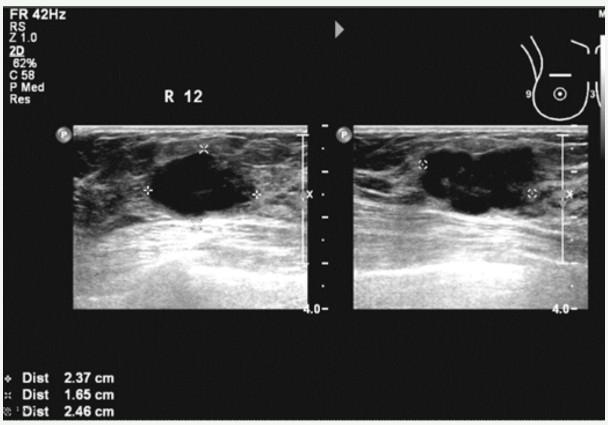

Figure 9. *Gray scale US at the upper mid part of right breast reveals a 2.4x1.6x2.5-cm oval circumscribed mixed hypo- and hyperechoic mass.*

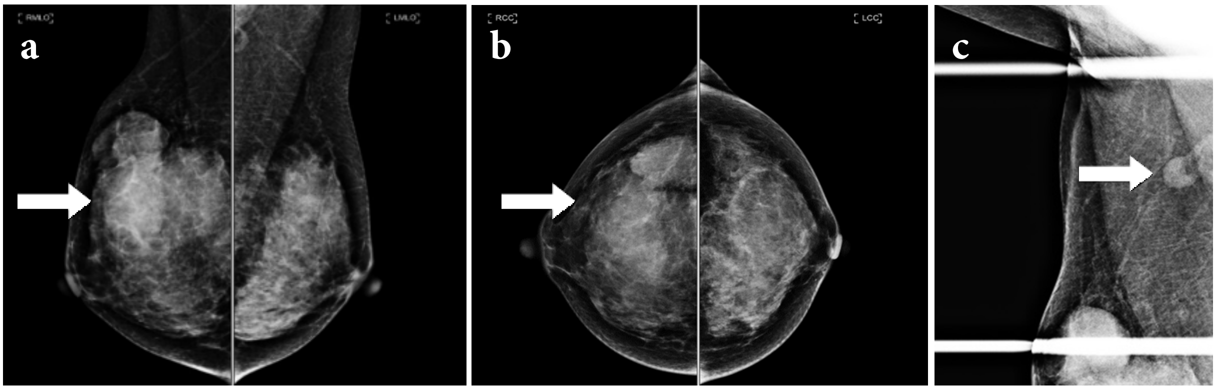

Figure 10. *Mammography (a) MLO (b) CC views of the right upper mid to the upper outer quadrant shows a large oval circumscribed mass with equal density at the right upper mid to the upper outer quadrant (arrow). (c) the right axillary view shows a few right axillary lymph nodes with thickened cortex (arrow).*

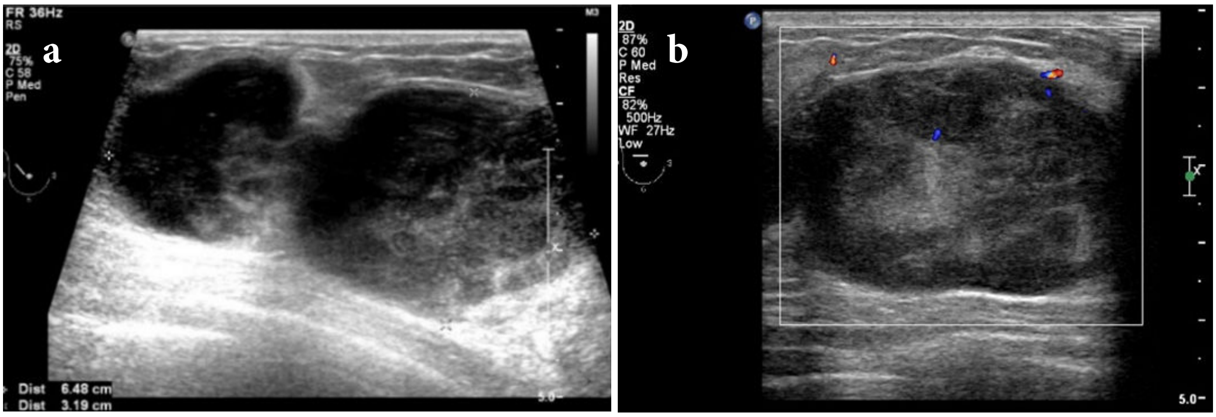

Figure 11. *Ultrasound (a) gray scale and (b) color doppler US at the right upper mid to the upper outer quadrant shows a 6.5x3.2x2.3 cm oval lobulated mixed hypo- and hyperechoic mass with minimal increased vascularity, which is increased in size from the initial study.*

Secondary breast lymphoma

Case 1

A 27-year-old female had a history of a painful palpable left breast lump for three months and purulent discharge from the left nipple. The mammography revealed enlargement of the left breast with global asymmetry, diffuse trabecular and skin thickening (Figure 12). US showed an irregular indistinct hypoechoic mass with hypervascularity occupying the central part of the left breast with a few adjacent smaller lesions and increased echogenicity of overlying subcutaneous fat (Figure 13). Several enlarged left axillary lymph nodes were also found. The condition was initially suspected for an infectious or inflammatory process such as breast abscess or idiopathic granulomatous mastitis. The patient was sent home with antibiotic treatment.

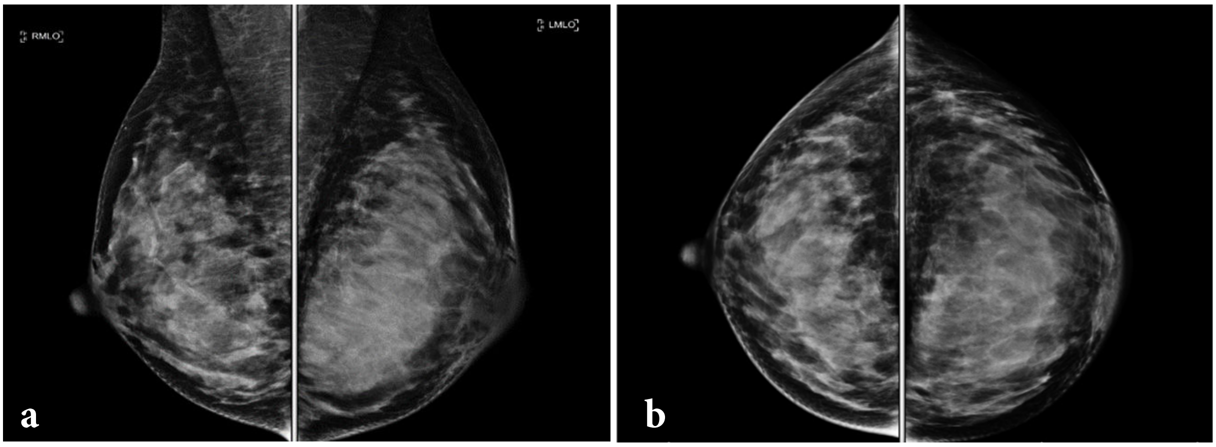

Figure 12. *Mammography (a) MLO (b) CC views shows enlargement of the left breast with global asymmetry, trabecular thickening and mild skin thickening involving nipple-areolar-complex.*

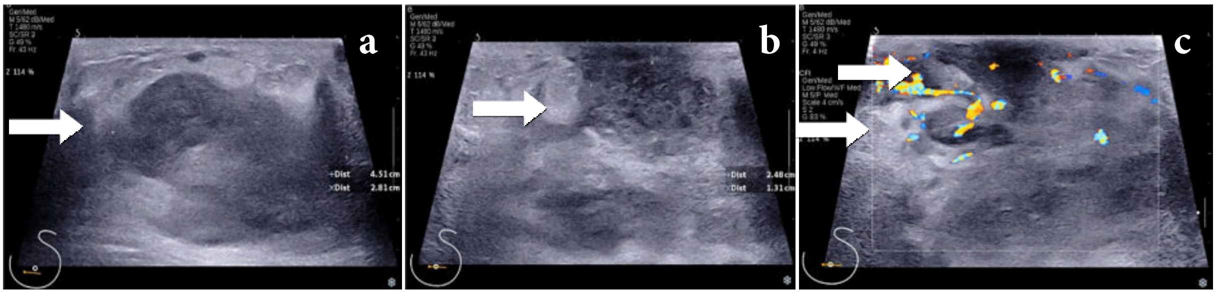

Figure 13. *Ultrasound (a) gray scale US at the central part of the left breast (b) gray scale and (c) color doppler US at the left subareolar region reveals an irregular indistinct hypoechoic mass with hypervascularity occupying the central part of left breast, about 4.5x2.8 cm, with a few indistinct smaller lesions at the left subareolar region (arrows).*

Follow-up US study about 2 weeks later revealed the increased size of a few irregular indistinct infiltrative hypoechoic masses at the left subareolar region and the left lower inner quadrant with a new lesion at the left outer mid part (Figure 14).

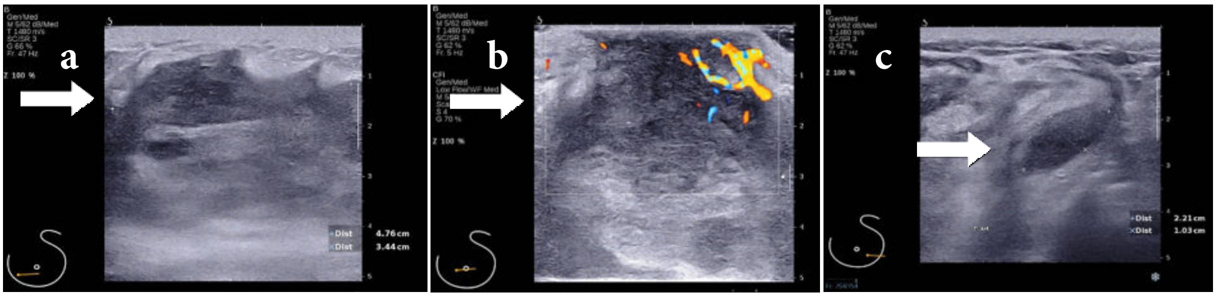

Figure 14. *Ultrasound (a) gray scale US at left lower inner quadrant and (b) left subareolar region reveals the increased size and extension of a few irregular indistinct infiltrative hypoechoic masses (arrows). Some liquefaction parts are suspected. (c) Gray scale US at the left outer mid part reveals a 2.2x1.0 cm new mass (arrow). There is surrounding increased echogenicity of subcutaneous fat and skin thickening.*

The patient underwent further breast MRI demonstrating multiple ill-defined conglomerated enhancing masses of various sizes occupying nearly the entire left breast, showing heterogeneous enhancement with type III kinetic curve (Figure 15). There were associated skin involvement and left nipple retraction. Multiple enlarged left axillary lymph nodes were seen.

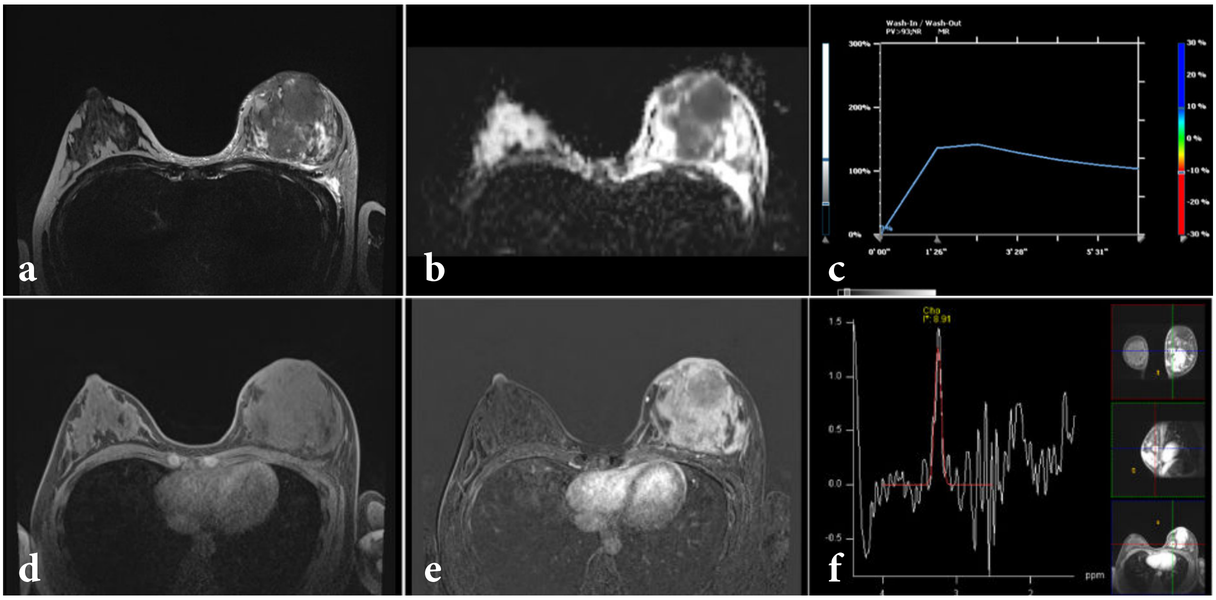

Figure 15. *MRI breast (a) T2-weighted axial image (b) ADC (c) Kinetic curve assessment (d) Fat-suppressed precontrast T1-weighted axial image (e) Fat-suppressed post contrast T1-weighted axial image with subtraction (delayed phase) (f) MR spectroscopy.*

There are multiple ill-defined conglomerate enhancing masses of various sizes occupying nearly the entire left breast, up to 5.0x4.4 cm, mainly at the left central region, showing isointensity on T1-weighted image, mild hyperintensity on T2-weighted image, heterogeneous enhancement with type III kinetic curve enhancement. The lesions show restricted diffusion (ADC 0.299x10^{-3}/mm^2) with elevated choline peak (8.91).

US-guided CNB of left breast mass confirmed diagnosis of DLBCL. CT scan of the chest revealed enlarged bilateral axillary and mediastinal lymph nodes and left pleural effusion. PET/CT after completion of chemotherapy demonstrated complete metabolic response of disease (Figure 16).

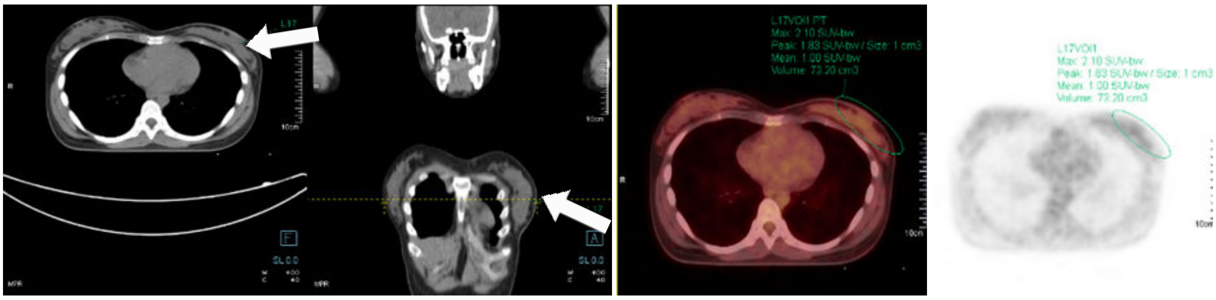

Figure 16. *PET/CT after completion of chemotherapy shows mild left fibroglandular tissue thickening with non-significant mild F-18 FDG uptake.*

Case 2

A 58-year-old female presented with a palpable left breast mass and bilateral axillary masses for six months. She also had generalized lymphadenopathy, weight loss and progessive dyspnea. The mammography revealed a partially obscured hyperdense mass at the left upper outer quadrant, US showing a round circumscribed hypoechoic mass with increased vascularity. Multiple bilateral axillary lymphadenopathies were seen (Figure 17 and 18). US-guided CNB of left axillary lymph nodes revealed follicular lymphoma. Staging CT examination also revealed multiple generalized lymphadenopathies, splenomegaly and bilateral pleural effusion. Bone marrow biopsy demonstrated disease involvement.

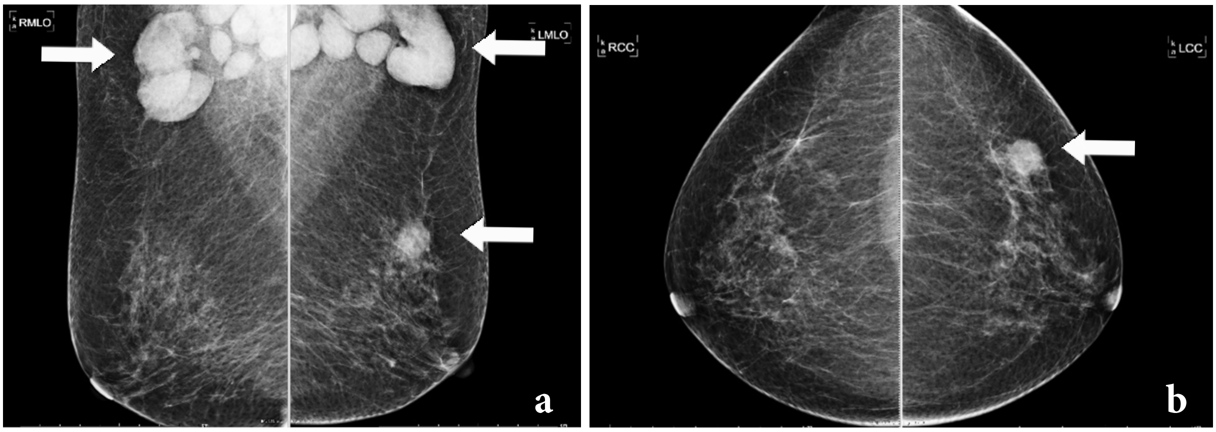

Figure 17. *Mammography (a) MLO (b) CC views reveals a 1.9x1.6x2.1-cm partially obscured hyperdense mass at the left upper outer quadrant. Multiple enlarged bilateral axillary lymph nodes are observed.*

Figure 18. *Ultrasound (a) gray scale US of the upper outer quadrant of the left breast shows a 1.4x1.1x1.5-cm circumscribed hypoechoic mass. Gray scale US at (b) left and (c) right axillary regions shows multiple bilateral axillary lymphadenopathies, up to 4.3 cm.*

Case 3

A 65-year-old female presented with mass in right nasal cavity for about six months. Biopsy of intranasal mass revealed DLBCL. Staging CT examination revealed several enhancing bilateral breast masses, several subcutaneous masses at the chest wall and the abdominal wall, right perinephric and gastric involvement (Figure 19).

The patient underwent mammography and US demonstrating several irregular indistinct masses at both breasts (Figure 20 and 21). No pathological examination of the breast masses was performed. Bone marrow biopsy revealed disease involvement. Mammography and US performed after 6th cycle of chemotherapy revealed the overall decreased size with some showed complete resolution of masses in both breasts.

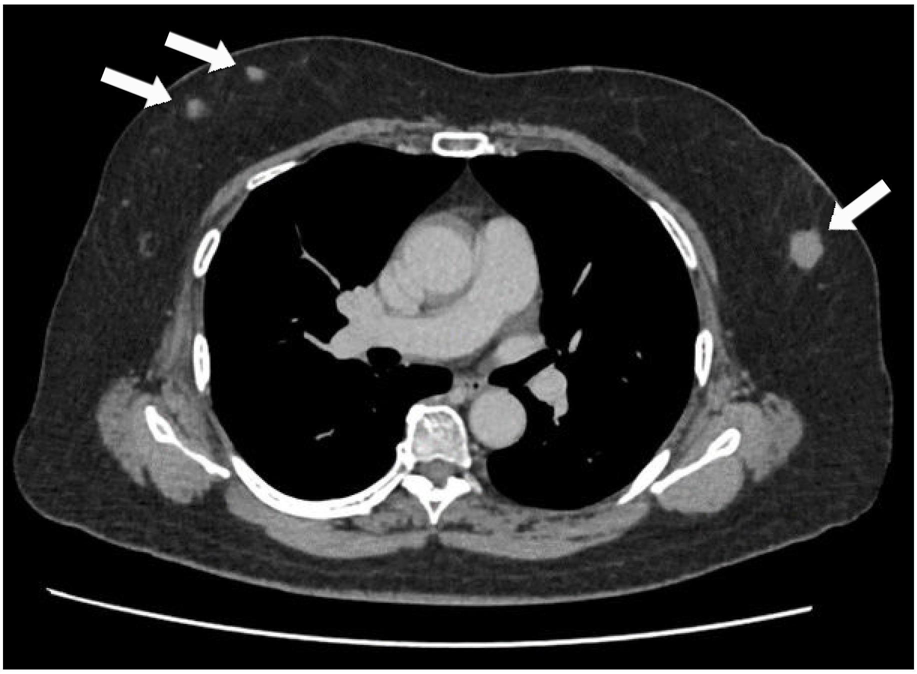

Figure 19. *Axial contrast enhanced CT scan of the chest shows several enhancing bilateral breast masses.*

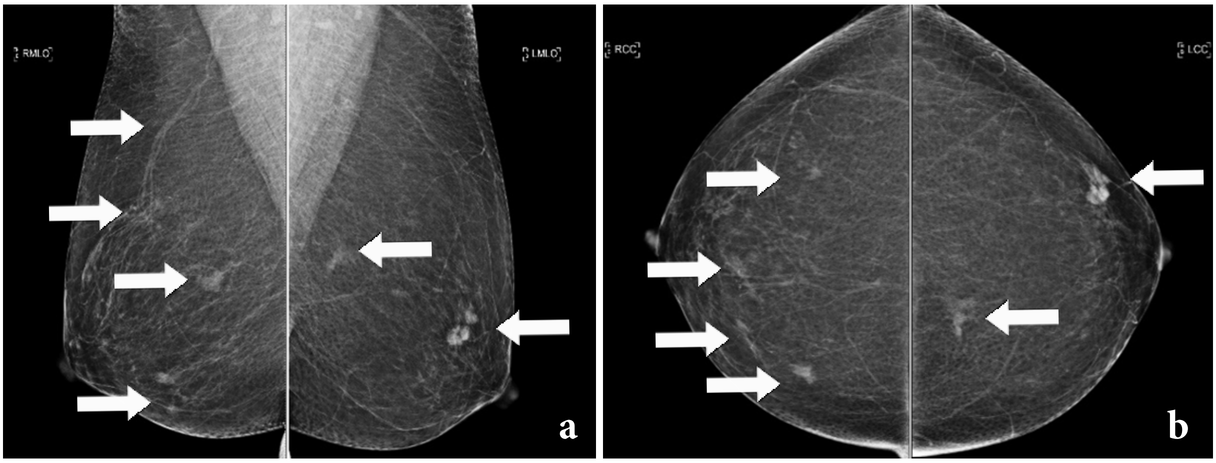

Figure 20. *Mammography (a) MLO (b) CC views reveal several irregular indistinct masses with equal and high density in both breasts.*

Figure 21. *Ultrasound gray scale US at (a) and (b) the outer mid part of the left breast (c) the lower mid part of right breast reveals several irregular indistinct hypoechoic masses in both breasts, up to 1.9x0.6x1.9 cm.*

Case 4

A 53-year-old female presented with a palpable left breast lump for one month. She denied of B symptoms. The mammography and US revealed circumscribed mass at the left lower inner quadrant (Figure 22 and 23). The patient underwent excisional biopsy which confirmed diagnosis of DLBCL. CT scan revealed liver dissemination.

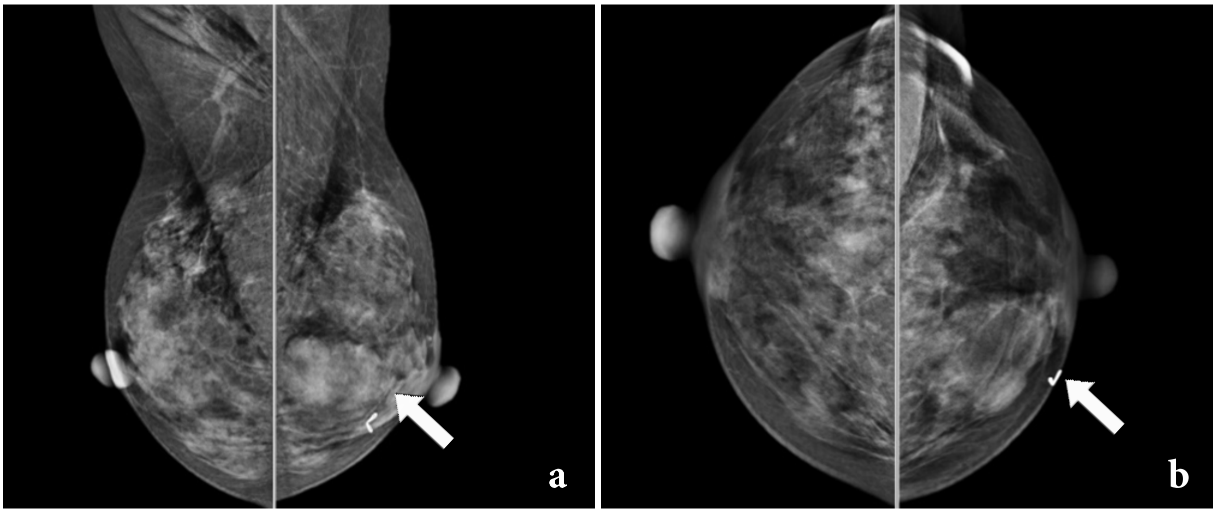

Figure 22. *Mammography (a) MLO (b) CC views reveal oval circumscribed mass with equal density at the left lower inner quadrant (arrow).*

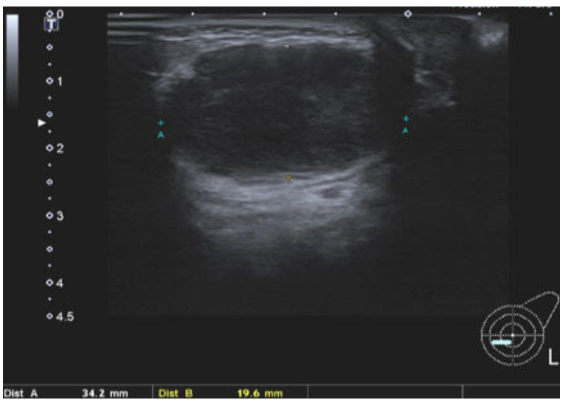

Figure 23. *Ultrasound gray scale US of lower inner quadrant of left breast shows a 3.4x2.0-cm oval circumscribed hypoechoic mass.*

Case 5

A 70-year-old female presented with a palpable left breast lump and a left axillary mass for three months. The mammography revealed a partially indistinct hyperdense mass at the left upper inner quadrant with skin and trabecular thickening (Figure 24), US showing a partially indistinct hypoechoic mass (Figure 25). Multiple enlarged left axillary lymph nodes were presented.

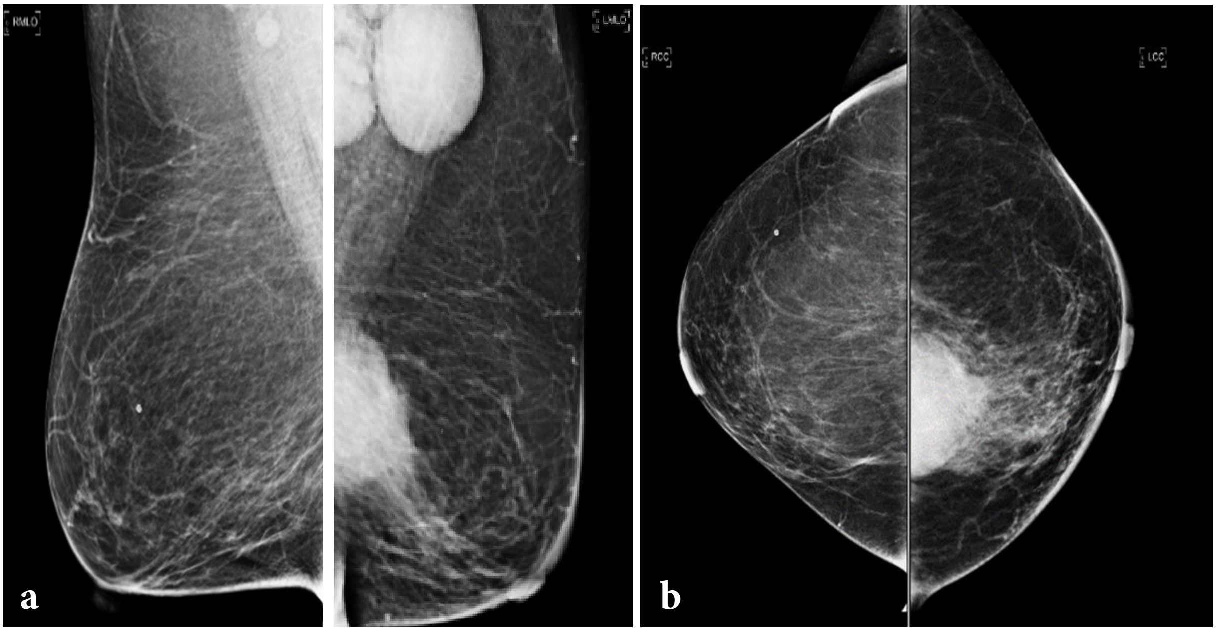

Figure 24. *Mammography (a) MLO (b) CC views reveal oval circumscribed mass with equal density at the left lower inner quadrant (arrow).*

THE ASEAN JOURNAL OF RADIOLOGY
ISSN 2672-9393

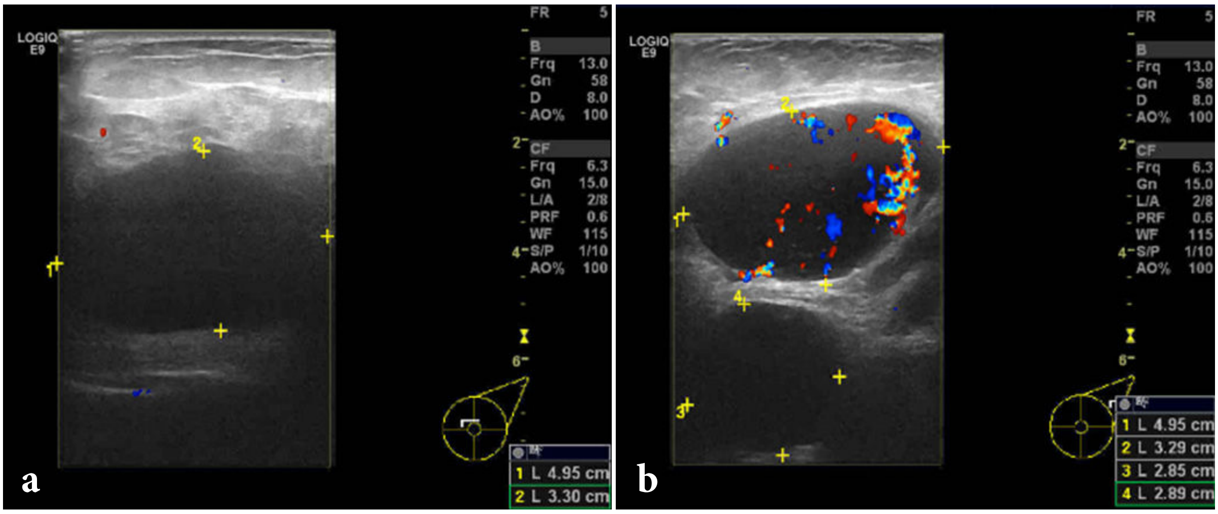

Figure 25. *Ultrasound (a) gray scale US of the upper inner quadrant of the left breast reveals a 5.0x3.3-cm round partially indistinct hypoechoic mass and (b) color doppler US at the left axilla reveals left axillary lymphadenopathy.*

The patient underwent breast MRI examination demonstrating a circumscribed thick rim-enhancing mass with type II kinetic curve pattern. The mass showed restricted diffusion and increased choline peak on MRS (Figure 26).

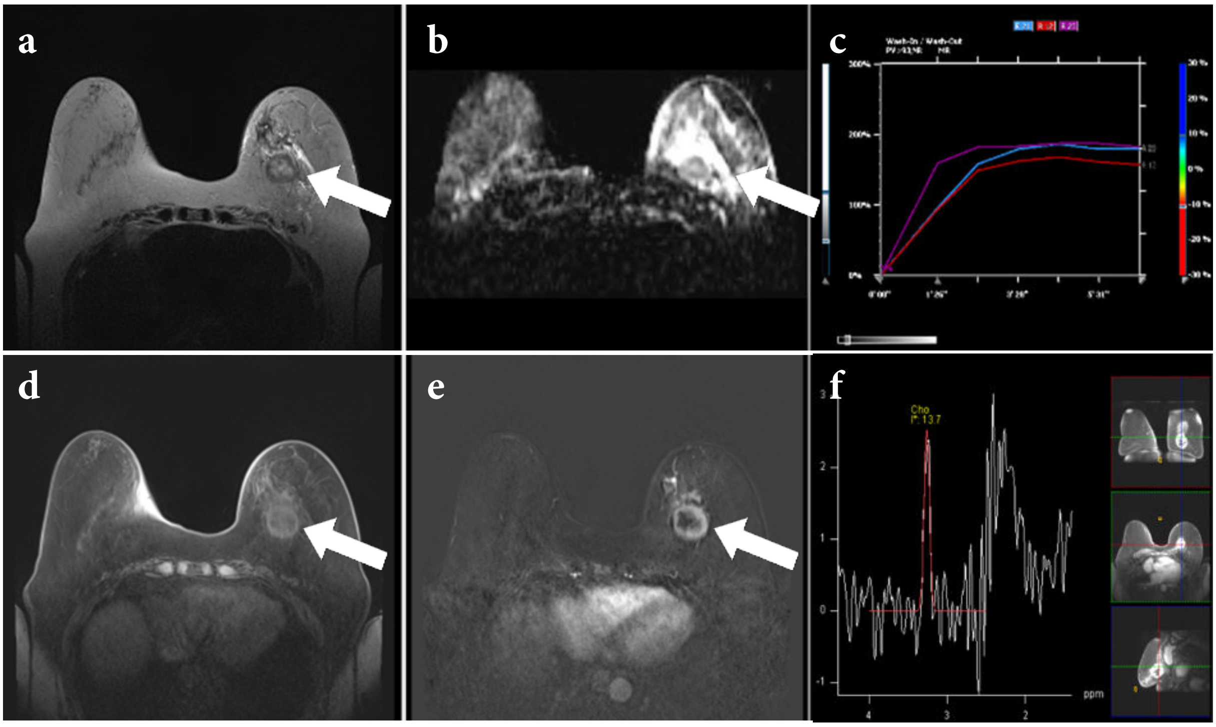

Figure 26. *MRI breast (a) T2-weighted axial image (b) ADC (c) kinetic curve assessment d. Fat-suppressed precontrast T1-weighted axial image (e) Fat-suppressed post contrast T1-weighted axial image with subtraction (delayed phase) (f) MR spectroscopy.*

Breast MRI reveals a circumscribed thick rim-enhancing mass at the left inner mid part, showing heterogeneous iso- to slight hypointensity on T1-weighted image, iso-to hyperintensity on T2-weighted image, irregular rim enhancement with type II kinetic curve pattern. The mass shows restricted diffusion (ADC 0.685x10-3/mm2) and an elevated choline peak on MRS (13.7).

The US-guided CNB of left axillary lymph node revealed DLBCL. Staging work-up revealed generalized lymphadenopathy, hepatic, splenic and bone marrow involvement. After completion of chemotherapy, there was an decreased size of the mass in the left breast with non-significant FDG-avidity, representing a complete metabolic response. PET/CT performed after complete remission for six months showed disease recurrence at the left breast, enlarged right external iliac nodes and inguinal nodes (Figure 27).

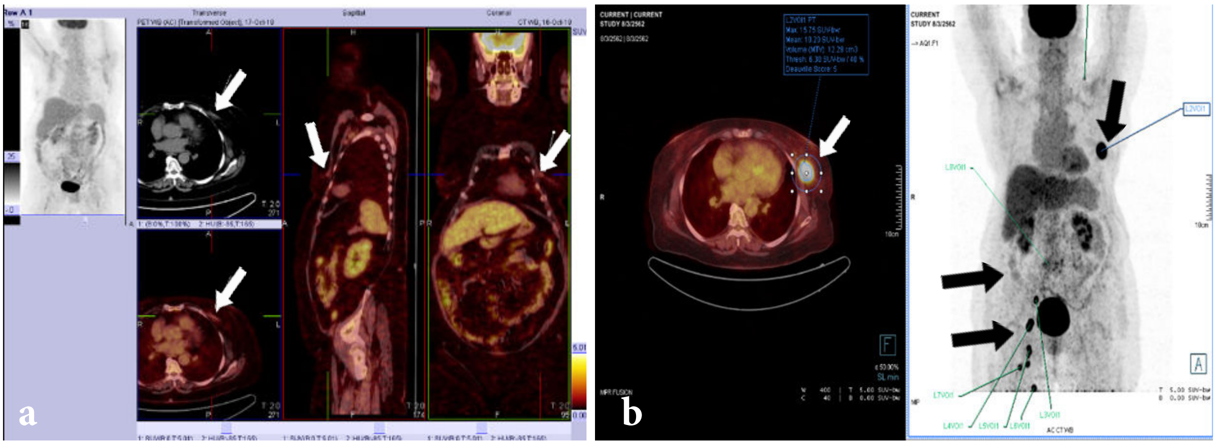

Figure 27. *(a) After completion of CMT, there was a decreased size non-significant FDG-avid mass in the left breast (arrows), representing a complete metabolic response. (b) PET/CT performed after complete remission for six months revealed a new 2.6x3.8x3.0-cm circumscribed FDG avid mass at the left breast (SUVmax =15.75), representing recurrence of disease.*

Discussion

Breast lymphoma is the rare manifestation of extranodal non-Hodgkin's lymphoma (NHL). We describe our experience of breast lymphoma seen at our institution including four cases of PBL and five cases of SBL.

Most of these cases presented with a painless palpable breast mass, except two cases of SBL: one with a painful breast mass and one with a right nasal mass. Five of the nine cases exhibited a palpable ipsilateral axillary lymph node including one of SBL cases who also had palpable contralateral axillary lymph node. Similar to the previous literature, the most common presentation of breast lymphoma is a painless enlarging palpable mass with minority of patients may exhibit pain (4-25%) and ipsilateral lymphadenopathy (30-40%) [1]. Other uncommon manifestations are breast enlargement, erythema, and edema [2,3]. Nipple retraction and nipple discharge are rare, unlike in breast carcinoma [1].

Solitary mass is the most common presentation in both PBL and SBL. Multiple masses are found in less than 10% and bilateral lesions are found in about 10%, which are more common in SBL [3,4]. Most of our patients exhibit a unilateral solitary breast mass and only one case of SBL had multiple bilateral breast masses.

One of our SBL cases reported weight loss, whereas none of PBL cases had any constitutional symptom. One case of SBL manifested with generalized lymphadenopathies. B symptoms are rarely associated with breast lymphoma, especially in PBL [2]. B symptoms and generalized lymphadenopathies may help suggesting the diagnosis of the secondary form.

The median age of the patients in this series was 58 years, ranging from 27 to 75 years, comparable with most common presenting age at 5th to 6th decades with a broad range of age reported in previous literature [2,4].

Various imaging modalities have a role in evaluation in breast lymphoma including mammography, ultrasonography (US), MRI and PET/CT scanning.

Mammography: The most common mammographic feature in our case series was a solitary breast mass with a circumscribed or indistinct margin. The masses were predominantly oval and round in shape. Most of the masses exhibited high and equal density while none of them exhibited calcifications. Less common features seen in our patients were global asymmetry and skin and trabecular thickening.

Similar findings have been reported in several studies. The most common presentation on mammography is a noncalcified solitary mass (69-72%). The mass is predominantly round or oval in shape and has an indistinct or circumscribed margin. Hyperdense appearance is depicted in more than 80% of breast lymphomas [3-5]. Less common features have been described, including multiple masses (3-9%), global asymmetry or diffuse increased density (9-16%), skin thickening or edema (up to 8%) or no abnormality on mammography (9%) [3-5].

Ultrasonography: Our patients mostly presented with an oval or irregular mass with circumscribed or indistinct margins, corresponding to the appearance on mammography. The mass was a hypoechogenic or mixed echogenic appearance. One of SBL who initially suspected of infectious/inflammatory condition demonstrated a marked hypoechoic appearance on US suspected of liquefied portion mimicking abscess. The vascularity assessed by doppler US was available in eight of our patients, all of which demonstrated increased vascularity. Associated posterior acoustic enhancement and no posterior acoustic features were seen. None of the patients demonstrated posterior acoustic shadow.

Our cases demonstrated comparable findings on US as mentioned in literature. Breast lymphomas usually present as hypoechoic or isoechoic masses with a circumscribed margin or a diffuse infiltrative appearance with indistinct margins. An almost anechoic mimicking fluid-filled lesion has also been described. The mass usually demonstrates increased vascularity at doppler US (55-64%) [4]. No acoustic feature or posterior acoustic enhancement is also a typical feature [5].

Surov et al found no significant differences in the mammographic or US features between PBL and SBL masses [5]. However, masses in PBL tend to have less number, less-defined margins, and a greater diameters than those observed in SBL [3,5].

Dynamic contrast material–enhanced MR imaging:
Breast MRI images were available in three of our patients (one case of PBL and two cases of SBL). Two cases showed circumscribed masses and one case showed ill-defined masses. All lesions exhibited heterogeneous iso-to slight hypointensity on T1-weighted image and heterogeneous hyperintensity on the T2-weighted image with heterogeneous or rim enhancement. All masses showed rapid initial increased signal intensity over 100% as compared with pre-contrast signal intensity. There was type II kinetic curve enhancement in two patients and type III in one patient. All masses showed restricted diffusion on ADC mapping. MR spectroscopy was performed in two patients which showed an elevated choline peak (8.91-13.7).

Our results were consistent with previous studies, with mass as the main appearance of breast lymphoma on MRI. The mass typically appears as iso to a hypointense mass on T1-weighted images, heterogeneously hyperintense on T2-weighted images, intense and heterogeneous enhancement. Type II kinetic curve enhancement is the most common pattern, followed by type III kinetic curve enhancement [4,5]. No significant differences in MRI features were detected between PBL and SBL [6]. MRI maybe useful in extension evaluation and detect multifocal and multicentric disease that might be underestimated on other imaging modalities.

PET/CT scan:
PET/CT scan has a role during initial staging of lymphoma, evaluating the treatment response or detecting recurrence of the disease. Intense hypermetabolism with F18–fluorodeoxyglucose (FDG) avidity is a typical feature, with a mean maximum SUV of 10.6 reported in the case series by Yang et al [4].

Two of our cases underwent PET/CT scan for evaluating the treatment response without a baseline pretreatment scan. PET/CT scan after completion of chemotherapy revealed a radiologically complete response. In one case of SBL, PET/CT scan had a role in detecting tumor recurrence, showing relapsed disease with a hypermetabolic activity at the left breast and distant lymph nodes.

There is no definite radiological difference between lymphoma and breast carcinoma. However, lymphoma should be considered as differential diagnosis of a mass lacking suspicious calcification, architectural distortion, spiculated border, or desmoplastic reaction on mammogram which are frequently seen in breast carcinoma [3,5]. Breast lymphoma typically does not exhibit posterior acoustic shadow on US which is a common feature in breast carcinoma [4].

Some particular clinical and radiological patterns help distinguish between the PBL and SBL (Table 1). Clinical or imaging finding of bilateral breast masses or bilateral axillary lymphadenopathy should raise concern about the presence of a secondary lymphoma. However, the causes of bilateral axillary lymphadenopathy are of broad range including leukemia, collagen vascular diseases, nodal hyperplasia, granulomatous diseases, human immunodeficiency viruses, and metastases.

Patients may present with clinical manifestations and imaging pattern mimicking inflammatory diseases. One case of SBL presented with a painful palpable breast mass accompanied with purulent nipple discharge and nipple retraction. The US examination revealed an irregular infiltrative lesion with a marked hypoechoic pattern resembling a fluid-filled lesion. The patient was initially misdiagnosed of an infectious or inflammatory breast condition. Complicated cysts with internal movable echoes or fluid-fluid level or fistulous tract toward skin are helpful features on US in differentiating the inflammatory condition from other breast conditions [6].

Histologic examination is essential for confirmation of diagnosis since the clinical and radiological features are not pathognomonic. Distinction of PBL from SBL also remains a diagnosis of exclusion which needs through diagnostic evaluation including staging CT examination, CSF examination and bone marrow biopsy [7].

Table 1. *Clinical and radiological patterns guide towards the primary and the secondary breast lymphoma.*

	PBL	SBL
Clinical presentation		
- Sign and symptom	palpable mass	palpable mass
- B symptoms	exceeding rare	may be present
- Multiplicity	unilateral, solitary	unilateral, solitary > multiple
- Axillary lymph node involvement	ipsilateral	ipsilateral or bilateral
- Generalized lymphadenopathy	none	may be present
- Previous diagnosis of hematologic malignancy	absence	may be present, breast mass representing metastatic or recurrent disease
Imaging		
Mammography, US, MRI	larger size, more indistinct margin	bilateral axillary lymphadenopathy multifocal, multicentric, bilateral lesions

Conclusion

This small case series illustrates the imaging spectrum of breast lymphoma presented at our institution. Despite the rarity, lymphoma should be considered as a differential diagnosis for the breast mass. Radiologic features combined with the clinical context and tissue diagnosis are essential for accurate diagnosis of lymphoma. Multimodality imaging also plays an important role in staging, follow-up, and detection of recurrence of breast lymphoma.

References

1. Domchek SM, Hecht JL, Fleming MD, Pinkus GS, Canellos GP. Lymphomas of the breast: primary and secondary involvement. Cancer 2002;94:6-13. doi: 10.1002/cncr.10163.

2. Brustein S, Filippa DA, Kimmel M, Lieberman PH, Rosen PP. Malignant lymphoma of the breast. A study of 53 patients. Ann Surg 1987;205:144-50. doi: 10.1097/00000658-198702000-00008.

3. Sabaté JM, Gómez A, Torrubia S, Camins A, Roson N, De Las Heras P, et al. Lymphoma of the breast: clinical and radiologic features with pathologic correlation in 28 patients. Breast J 2002;8:294-304. doi: 10.1046/j.1524-4741.2002.08509.x.

4. Yang WT, Lane DL, Le-Petross HT, Abruzzo LV, Macapinlac HA. Breast lymphoma: imaging findings of 32 tumors in 27 patients. Radiology 2007;245:692-702. doi: 10.1148/radiol.2452061726. Epub 2007 Oct 2.

5. Surov A, Holzhausen HJ, Wienke A, Schmidt J, Thomssen C, Arnold D, et al. Primary and secondary breast lymphoma: prevalence, clinical signs and radiological features. Br J Radiol 2012;85:e195-205. doi: 10.1259/bjr/78413721.

6. Lepori D. Inflammatory breast disease: The radiologist's role. Diagn Interv Imaging 2015;96:1045-64. doi: 10.1016/j.diii.2015.07.006. Epub 2015 Sep 12.

7. Wiseman C, Liao KT. Primary lymphoma of the breast. Cancer 1972;29:1705-12. doi: 10.1002/1097-0142(197206)29:6<1705::aid-cncr2820290640>3.0.co;2-i.

Case Report

Regression of lung bullae after pulmonary infection: Two case reports and the aspect of radiologic and pathologic findings in one case

Pachayree Booncharoen, M.D.[1]
Tanaporn Eiambanapong, M.D.[1]
Tanapol Jiwanan, M.D.[1]
Kanet Kanjanapradit, M.D.[2]
From [1] Department of Radiology and [2] Department of Pathology, Faculty of Medicine, Prince of Songkla University, Songkla, Thailand.
Address correspondence to P.B. (e-mail: pachayree.b@gmail.com)

Received 4 April 2022 ; revised 9 August 2022 ; accepted 12 August 2022
doi:10.46475/aseanjr.v23i2.169

Abstract

A sharply demarcated area of emphysema, bleb or bulla, is usually asymptomatic. Some could lead to pneumothorax or superimposed infection, the common complications, while some could be spontaneously resolved, of which mechanism remains unclear.

We present two male patients who had asymptomatic bullae at their right upper lungs. The first patient presented with a low-grade fever for a month. His chest radiograph showed a new patchy opacity in right upper lung, which corresponds to an enhancing mass with central necrosis on the chest computed tomography. His tissue pathology from two specimens of pleura had proven as inflammation and fibrosis. After antibiotics treatment, the follow-up images showed partial regression of the bullae. Another patient presented with right pleuritic chest pain for 16 days and was diagnosed as pneumonia with an infected lung bulla. His chest radiograph showed a newly seen patchy opacity at the right middle lung zone and a new air-fluid level in the lung bulla in the right upper lobe. After he had been given antibiotics treatment, partial regression of the bulla was observed. He later underwent right upper lobectomy and successful smoking cessation. The follow-up chest images showed no new bleb or bulla.

Keywords: Bulla, Bleb, Spontaneous regression, Infection.

Case summary

A 68-year-old Thai male, former smoker of 150 packs a year with underlying chronic obstructive pulmonary disease, has been treated with the inhaled beta-agonist and corticosteroid therapy. He was clinically well-controlled and rarely had an acute exacerbation. The patient has also had asymptomatic right apical lung bullae since 2013 (Figure 1A).

In February 2018, the patient presented with a dry cough with a low-grade fever for a month. His chest radiograph revealed a new patchy opacity at the right upper lobe (RUL) with a cavitary-like lesion (Figure 1B). The physical examination showed expiratory wheezing in both lungs. Three sputum smears for acid-fast bacillus were all negative. He was suspected for having lung cancer; therefore, chest computed tomography (CT) was scheduled and later showed the centrally necrotic enhancing mass surrounding by reticulofibrosis and multiple bullae, suspected of apical lung bronchogenic carcinoma or scar carcinoma (Figure 2). Tissue biopsy was performed and revealed areas of lymphocyte infiltration and fibrous bands representing acute and chronic inflammation and fibrosis (Figure 3). In the meantime, he was treated with antibiotics as amoxicillin/clavulanate potassium for seven days.

In April 2018, his symptoms were improved and the follow-up chest radiograph revealed only the right apical pleural thickening (Figure 1C, 1D).

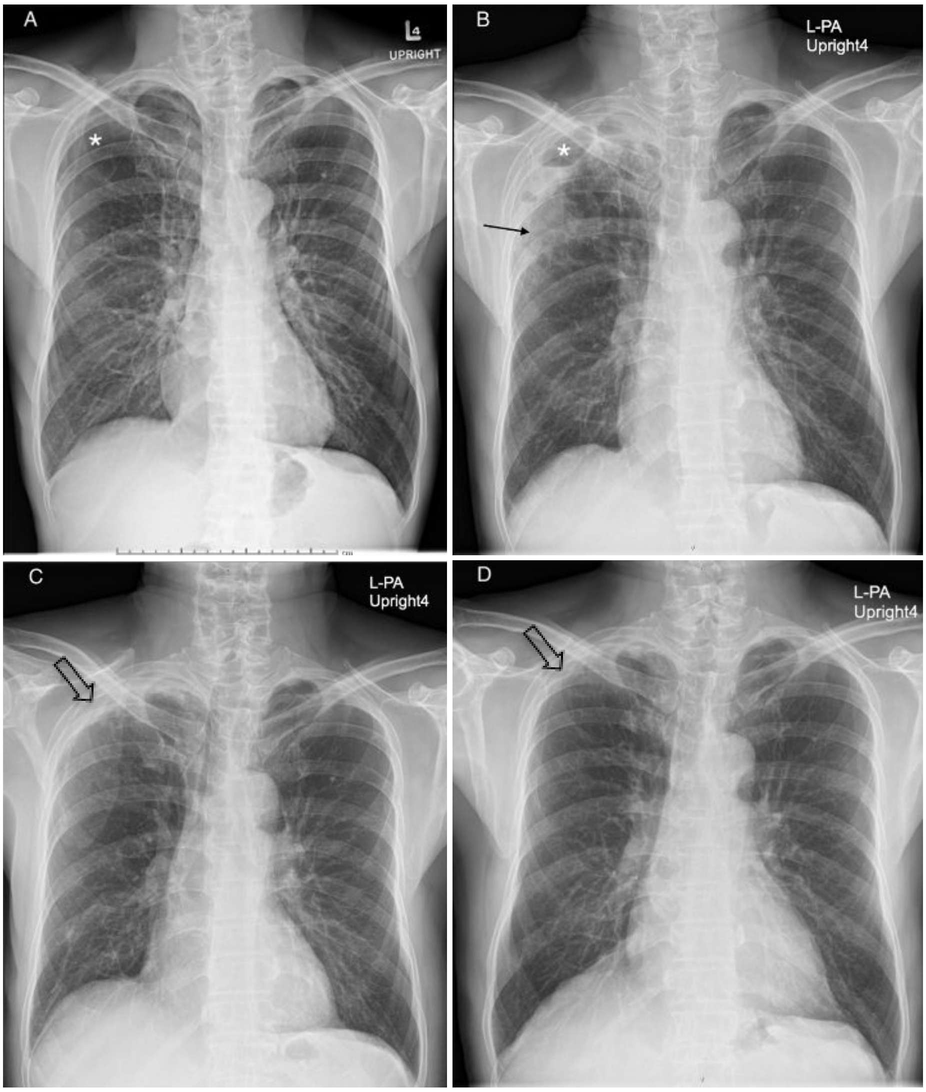

Figure 1. *Chest radiograph PA upright in 2013 (A) shows a thin-wall air-filled cavity compatible with a bulla in the RUL (asterisk). In February 2018, chest radiograph (B) shows the previously seen bulla (asterisk) with a new surrounding patchy opacity (black arrow). The follow-up chest images after treatment in March 2018 (C) and in December 2020 (D) show smaller size of the cavitary lesion with gradually improved right apical pleural thickening (open arrows), compatible with partial regression of the lung bullae.*

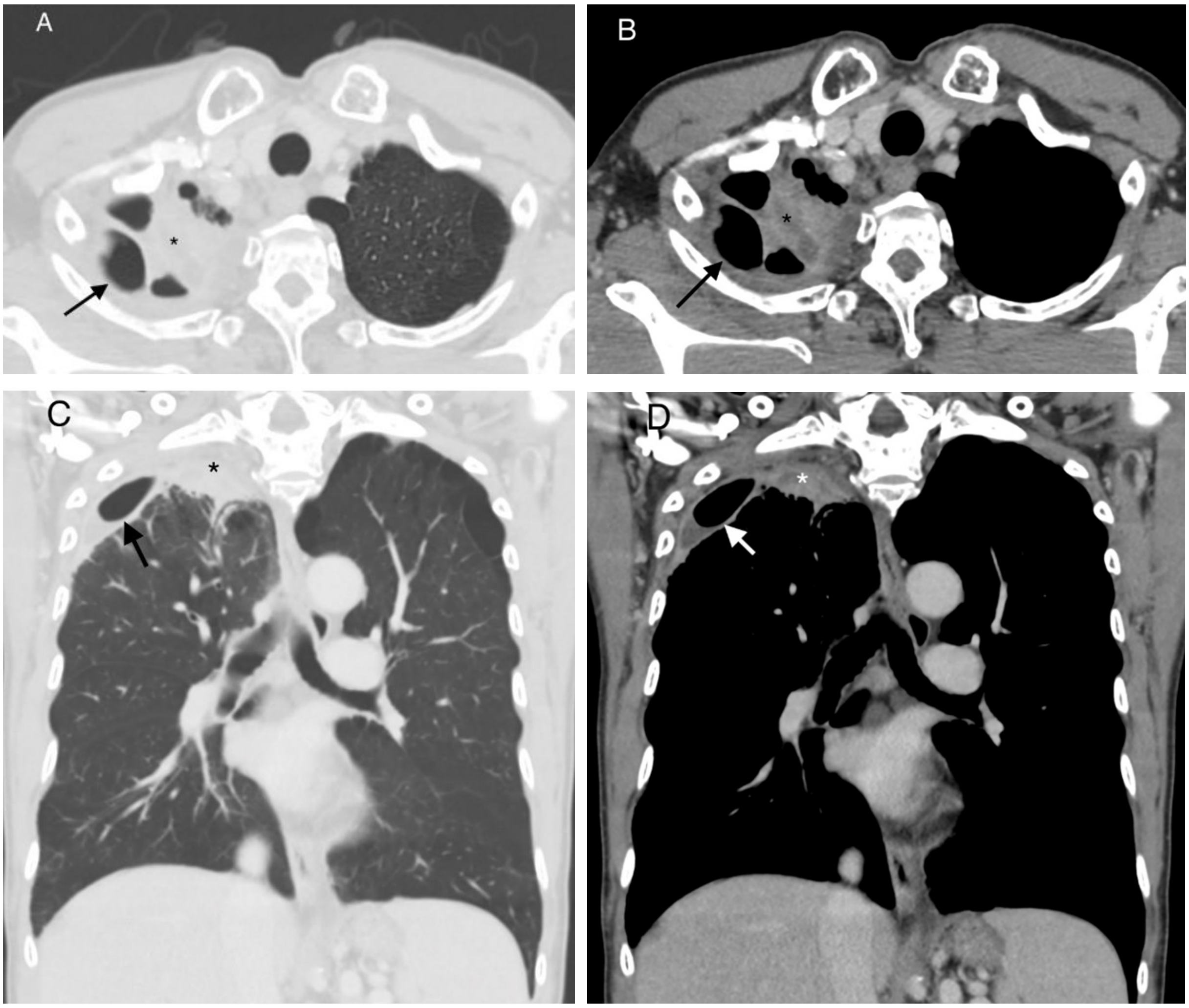

Figure 2. *Conventional CT of the chest in axial (A, B) and coronal views (C, D) in lung window (A, C) and mediastinum window (B, D) shows an enhancing mass with central necrosis in the right apical lung (asterisks) and multifocal cavity (arrows).*

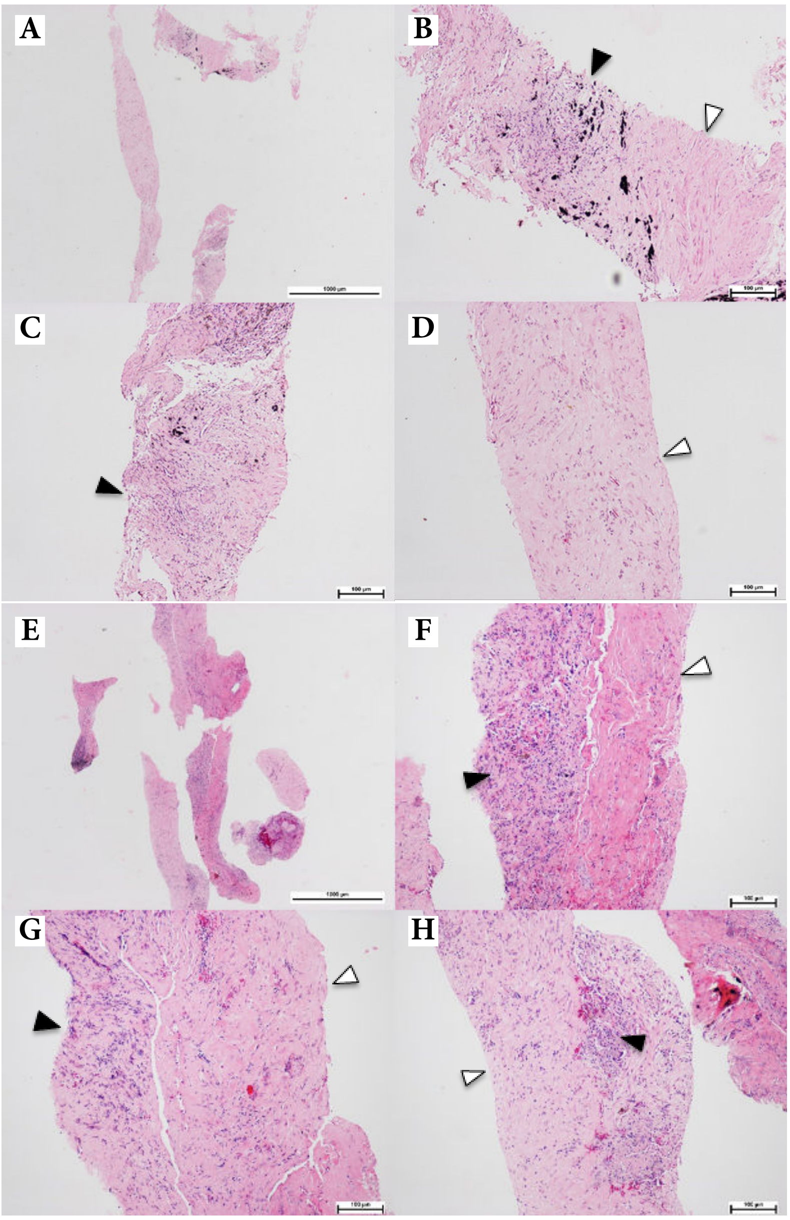

Figure 3. *Core biopsy from pleura number 1(A-D): (A) 40x magnification, (B) 100x magnification shows area of lymphocyte infiltration (black arrow head) representing chronic inflammation, and an area of the fibrous band (white arrow head), (C) 100x magnification shows an area of lymphocyte infiltration (black arrow head), and (D) 100x magnification shows the fibrous band (white arrow head). No malignant cell is demonstrated. Core biopsy from pleura number 2 (E-H): (E) 40x magnification and (F-H) 100x magnification show an area of lymphocyte infiltration, representing chronic inflammation(black arrow head), and an area of fibrous band without a malignant cell (white arrow head). All specimens are stained in hematoxylin-eosin.*

In August 2021, the patient developed worsening oxygenation. The high-resolution computed tomography (HRCT) of the chest was scheduled in order to evaluate the possible causes, such as interstitial lung disease. The study confirmed the regression of the RUL bullae (Figure 4).

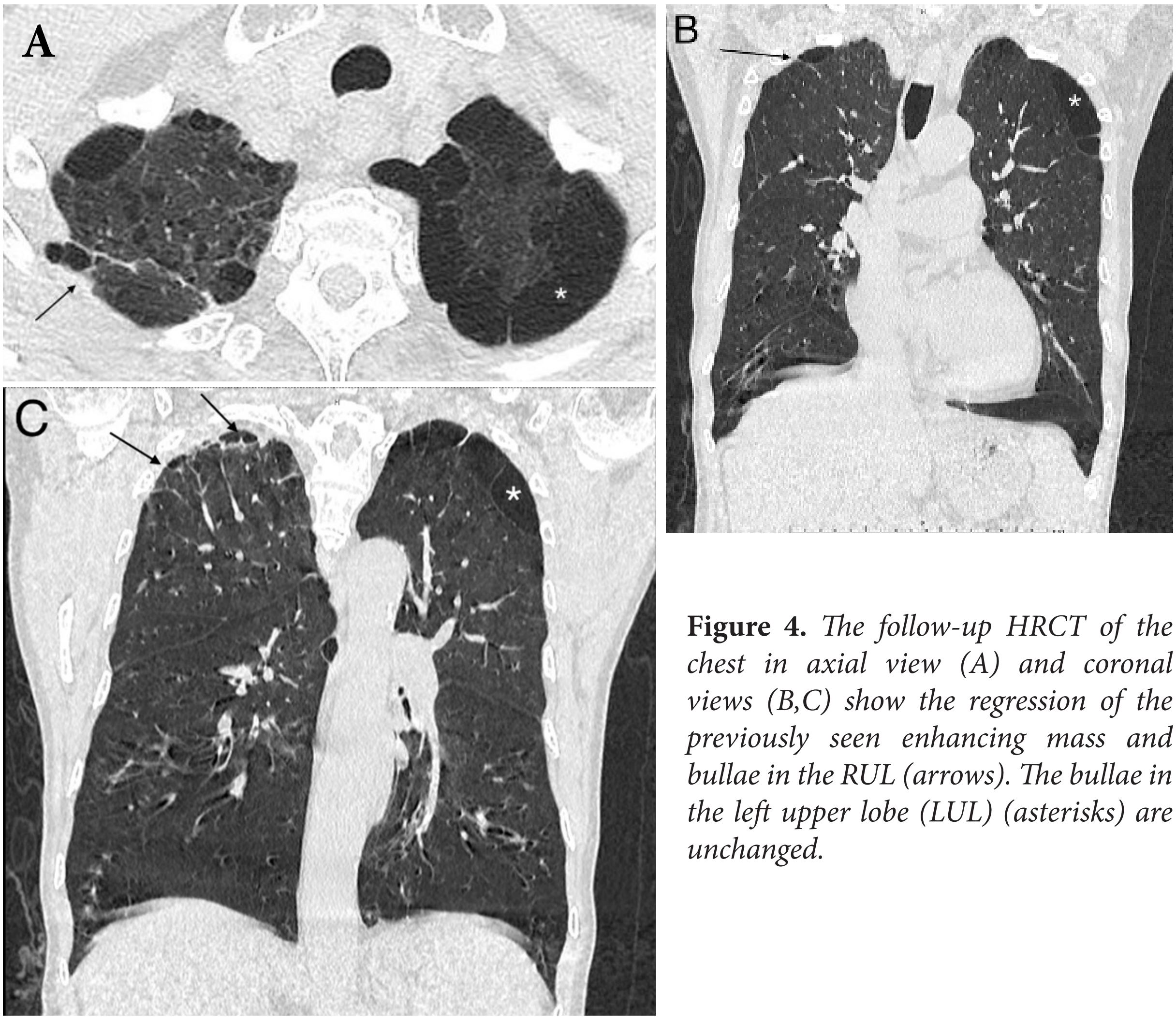

Figure 4. *The follow-up HRCT of the chest in axial view (A) and coronal views (B,C) show the regression of the previously seen enhancing mass and bullae in the RUL (arrows). The bullae in the left upper lobe (LUL) (asterisks) are unchanged.*

Our second patient, a 64-year-old male smoker of 40 packs a year with underlying gouty arthritis presented with right pleuritic chest pain for 16 days in September 2012. He also had fever and productive cough for 10 days. The physical examination revealed bilateral coarse crepitation at both lower lungs. His chest radiograph (Figure 5B) showed a newly seen patchy opacity at RUL and a new air-fluid level in the previously seen RUL bulla since 2011 (Figure 5A), which preoccupied almost one third of the right hemithorax. He was diagnosed with pneumonia with an infected lung bulla, and was given a 1-gram tablet of amoxicillin /clavulanate potassium twice daily with other supportive medication. The chest CT was scheduled for full evaluation. At the time, the patient denied undergoing bullectomy.

A week later, the chest CT (Figure 6) revealed a thin-walled cavity at the apical segment of RUL with a smooth internal margin with an internal air-fluid level (corresponding with the previous chest radiograph), minimal residual reticulonodular infiltration at the posterior segment of RUL, and minimal cylindrical bronchiectasis with ground-glass opacity at the superior segment of the right lower lobe (RLL). Resolving pneumonia and infected RUL bulla were confirmed.

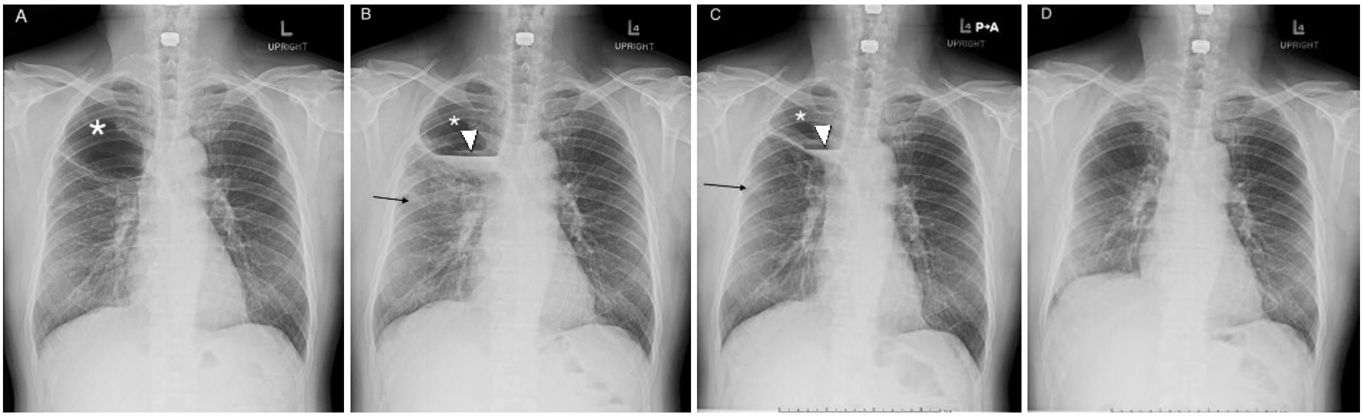

Figure 5. *Baseline chest radiograph (A) in 2011 indicated to work up the secondary cause of his arthralgia, an asymptomatic lung bulla (asterisk) is seen as an air-filled cavity, about 10.2x8.9 centimeters in size, at the RUL. The workup chest radiograph for the right pleuritic chest pain in September 2012 (B) shows a newly seen patchy opacity at RUL (arrow) and a new air-fluid level in the previous bulla in the RUL (arrow head). The diagnosis of pneumonia with an infected bulla at RUL is made. The follow-up chest radiograph after two weeks of antibiotic treatment (C) shows the decreased RUL bulla's size from the baseline (asterisk) that was about 8.4x8.3 centimeters in dimension, and a decreased amount of internal fluid (arrow head), suggestive of spontaneous partial regression of the bulla. Also, a noted disappearance of patchy opacity at RUL, likely resolved pneumonia (arrow). Finally, after discussion with cardiothoracic surgeon about the residual bulla, this patient underwent RUL lobectomy three months later without a serious post-operative complication. The post operative follow-up chest radiograph in January 2013 (D) reveals the right apical pleural thickening of surgical change and no residual bullae with mild decreased right lung volume.*

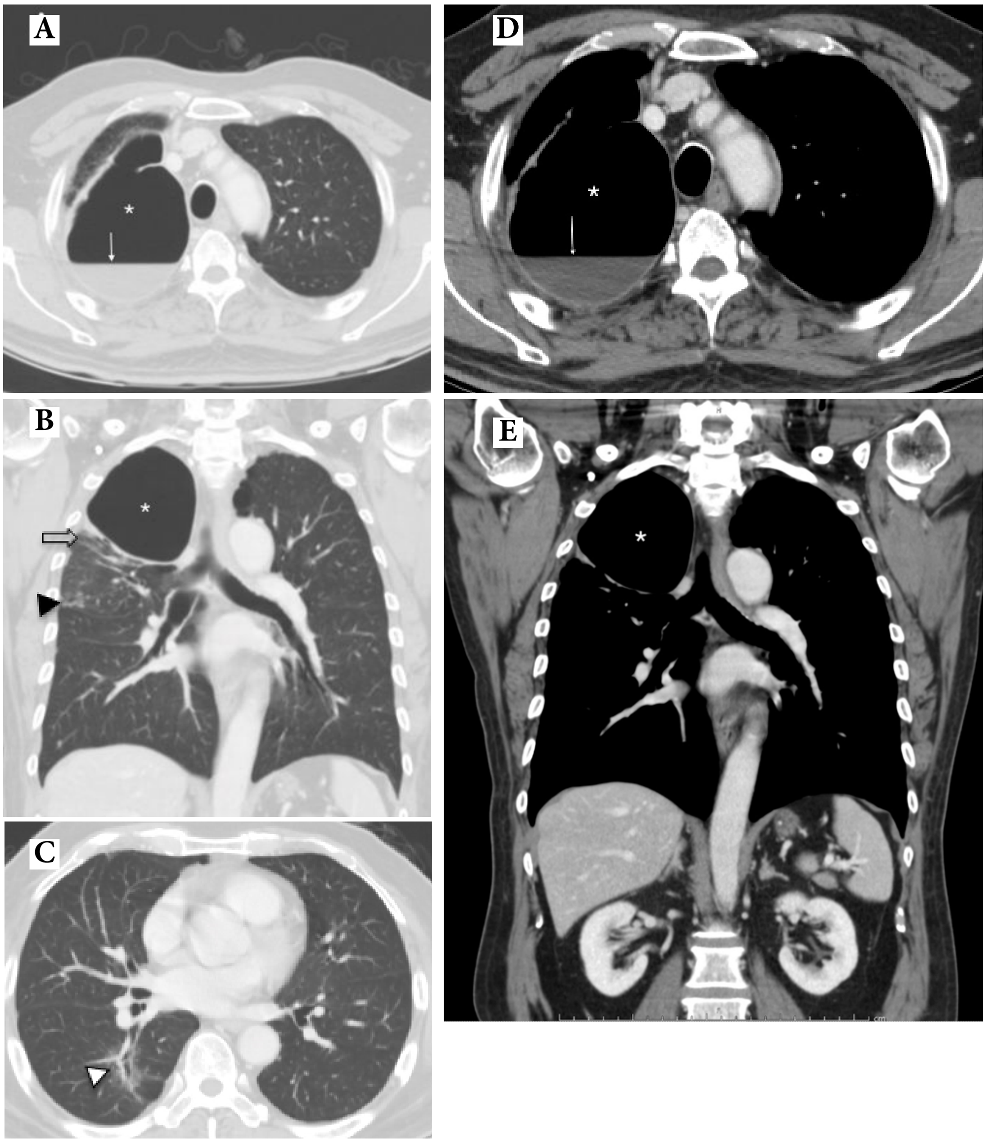

Figure 6. *The contrast enhanced CT of the chest for full evaluation of infected lung bulla in axial (A,C,D) and coronal views (B,E) of the lung window (A,B,C) and the mediastinal window (D,E) eight days after the treatment shows a thin-walled cavitary lesion at the apical segment of the RUL (asterisks) with a smooth internal margin and an internal air-fluid level (arrows in A,D), corresponding with the air-fluid level in the bulla on figure 4B. A small area of the centrilobular nodules in RUL (black arrow head in B) corresponding with the patchy opacity in figure 5B and 5C, and minimal residual reticulonodular infiltration at the posterior segment of RUL (open arrow in B), and minimal cylindrical bronchiectasis with ground-glass opacity at the superior segment of RLL (white arrow head in C) confirmed the resolving pneumonia.*

At 2-week follow-up after the first visit, his symptoms subsided including afebrile and less dyspnea. The chest image (Figure 5C) showed disappearing patchy opacity at RML, likely resolved pneumonia. The RUL bulla had a decreased amount of internal fluid and a smaller size than on the baseline chest radiograph in 2011. The patient agreed to visit the cardiothoracic surgeon, and the antibiotic treatment was discontinued.

In December 2012, the patient underwent RUL lobectomy at a new hospital. He came to the outpatient department of the cardiothoracic surgery for post-operative follow-up in January 2013 without a serious complication. The follow-up chest radiograph showed no residual cavitary-like lesion (Figure 5D). In addition, he reported successful smoking cessation.

Discussion

Bullae, the gas-containing spaces, usually are well-defined emphysematous areas larger than 1 cm in diameter with walls less than 1 millimeter thick [1]. These commonly found gas-containing spaces are usually accompanied by the emphysematous changes of the adjacent lung.

Patients with a lung bulla usually are asymptomatic, but some may develop complications, namely, pneumothorax, superimposed infection, hemorrhage, or bronchogenic carcinoma [2-4]. The treatment of the symptomatic bulla includes smoking cessation or surgical management in patients with refractory dyspnea due to a giant bulla, which is arbitrarily defined as one that occupies at least one third of the volume of a hemithorax [2]. A spontaneous decrease in size of the bullous lesions has been reported in only 4 of 49 patients during the x-ray follow-ups [4], of which the mechanism still remains unclear. According to the literature review by Chang [5], the spontaneous regression and resolution of giant bullae in most cases could occur after infection or smoking cessation. Although the pathophysiology of this resolution has not been well understood, the airway inflammation is believed to cause obliteration of the communication between the airway and the bullae. When the bullae become close spaces, the internal air might have been absorbed resulting in their regression.

Some authors have also reported about the spontaneous regression of giant bullae after smoking cessation and the intensive care with an inhaled bronchodilator and anti-inflammatory medication. To our knowledge, tobacco smoke could increase airway inflammation; therefore, smoking cessation could decrease airway inflammation and obstruction, as well as anti-inflammatory medication, which results in bulla regression.

Our patient, a former smoker of 150 packs a year, presented with a dry cough and a low-grade fever for a month. The chest CT showed focal reticulofibrosis near the prior RUL bulla could be related to the tissue pathology showing areas of fibrous bands, while patchy or ground glass opacities could be related to areas of lymphocyte infiltration from acute and chronic inflammation. After he was previously treated with the inhaled corticosteroid and recently treated with antibiotics, the disappearance of the bullae in his follow-up chest HRCT might be the result of the prior infection or inflammatory process.

Theoretically, emphysema is a condition characterized by permanent enlargement of the respiratory airspaces accompanied with destruction of their walls without obvious fibrosis [6-8], granulation tissue, or inflammation [9]. The presence of lymphocytes and collagen in the wall of the bulla in one of our cases is likely the result of chronic infection and could be responsible for its spontaneous regression. However, cystic lesions found in smokers other than emphysema such as airspace enlargement with fibrosis are pathologically defined with dense fibrous walls [10] and scanty inflammatory cells [9]. Paraseptal emphysema, which is less comprehensively studied comparing to other kinds of emphysema, was mentioned to associate with a dense fibrous wall in one study [11].

In the second patient, a 64-year-old male smoker of 40 packs a year, the period of the infection was more specific and evident on the series of chest images. Spontaneous partial regression was also observed during the antibiotic treatment. About seven months after the beginning of smoking cessation and one month after the right upper lobectomy was performed, there was no new bleb or bulla on the follow-up chest films. This could imply that the spontaneous partial regression may be associated with previous infection/inflammation or smoking cessation. The disadvantages of this case were that the pathological result was not available to explain the correlation with the radiographic findings; also, the details of the smoking cessation were not available on the medical records.

Furthermore, the bulla in this case, which occupied almost one third of right hemithorax, could be defined as a giant bulla. Eleven cases of complete resolution and six cases with partial regression of giant bullae are reported [12]. The bullectomy was offered to the patient despite the partial regression of the bulla in the follow-up chest radiograph. Otherwise, according to Mehran's study [13], if a patient has a smaller bulla, which is less than 30% of the volume of the hemithorax, the dyspnea is unlikely to be related to the bulla and its excision is probably not indicated.

This case report supports those factors such as prior infection or an inflammatory process, smoking cessation, and anti-inflammatory medication in some cases, relate to the spontaneous resolution of the bullae. As mentioned in Daewa et al [14], the pathophysiology of this mechanism has still not been completely understood. A further study or observation is still needed to ensure the relation between bulla regression and these factors.

References

1. Hansell DM, Bankier AA, MacMahon H, McLoud TC, Müller NL, Remy J. Fleischnersociety: glossary of terms for thoracic imaging. Radiology [Internet] 2008 [cited 2022 Jan 16];246:697–722. Available from: https://pubs.rsna.org/doi/10.1148/radiol.2462070712 Subsciption required.

2. Webb WR, Higgins CB. Thoracic imaging: pulmonary and cardiovascular radiology. 2nd ed. Philadelphia: Lippincott Williams & Wilkins; 2011.

3. Arab WA, Echavé V, Sirois M, Gomes MM. Incidental carcinoma in bullous emphysema. Can J Surg [Internet] 2009 [cited 2022 Jan 16]; 52: E56-7. Available from: https://www.ncbi.nlm.nih.gov/pmc/articles/PMC2689732

4. Boushy SF, Kohen R, Billig DM, Heiman MJ. Bullous emphysema: clinical, roentgenologic and physiologic study of 49 patients. Dis Chest [Internet] 1968 [cited 2022 Jan 16]; 54: 327–34. Available from: https://www.sciencedirect.com/science/article/pii/S0096021715342916?via%3Dihub Subsciption required.

5. Chang WH. Complete spontaneous resolution of a giant bulla without rupture or infection: a case report and literature review. J Thorac Dis [Internet] 2017 [cited 2022 Jan 16]; 9: E551-5. Available from: https://jtd.amegroups.com/article/view/13851

6. The definition of emphysema. Report of a National Heart, Lung, and Blood Institute, Division of Lung Diseases workshop. Am Rev Respir Dis [Internet] 1985 [cited 2022 Aug 08]; 132: 182-5. Available from: https://www.atsjournals.org/doi/10.1164/arrd.1985.132.1.182 Subsciption required.

7. Snider GL. Emphysema: the first two centuries—and beyond. A historical overview, with suggestions for future research: Part 1. Am Rev Respir Dis [Internet] 1992 [cited 2022 Aug 08]; 146:1334-44 Available from: https://www.atsjournals.org/doi/abs/10.1164/ajrccm/146.5_Pt_1.1334 Subsciption required.

8. Snider GL. Emphysema: the first two centuries—and beyond. A historical overview, with suggestions for future research: Part 2. Am Rev Respir Dis [Internet] 1992 [cited 2022 Aug 08]; 146: 1615–22. Available from: https://www.atsjournals.org/doi/10.1164/ajrccm/146.6.1615 Subsciption required.

9. Yamada T, Nakanishi Y, Homma T, Uehara K, Mizutani T, Hoshi E, et al. Airspace enlargement with fibrosis shows characteristic histology and immunohistology different from usual interstitial pneumonia, nonspecific interstitial pneumonia and centrilobular emphysema. Pathol Int [Internet] 2013; [cited 2022 Aug 08]; 63: 206-13. Available from: https://onlinelibrary.wiley.com/doi/10.1111/pin.12054 Subsciption required.

10. Lin H, Jiang S. Combined pulmonary fibrosis and emphysema (CPFE): an entity different from emphysema or pulmonary fibrosis alone. J Thorac Dis [Internet] 2015 [cited 2022 Aug 08]; 7: 767-79. Available from: https://www.ncbi.nlm.nih.gov/pmc/articles/PMC4419325/

11. Pipavath SN, Schmidt RA, Takasugi JE, Godwin JD. Chronic obstructive pulmonary disease: radiology-pathology correlation. J Thorac Imaging [Internet] 2009 [cited 2022 Aug 08]; 24: 171-80. Available from: https://journals.lww.com/thoracicimaging/Fulltext/2009/08000/Chronic_Obstructive_Pulmonary_Disease_.4.aspx

12. Ryland PB Jr, Thomas MR. Spontaneous partial resolution of a giant pulmonary bulla. Austin J Pulm Respir Med [Internet] 2014 [cited 2022 April 13];1: 1017. Available from: https://austinpublishinggroup.com/pulmonary-respiratory-medicine/fulltext/ajprm-v1-id1017.php

13. Mehran RJ, Deslauriers J. Indications for surgery and patient work-up for bullectomy. Chest Surg Clin N Am [Internet] 1995 [cited 2022 April 13]; 5: 717-34. Available from: https://www.scopus.com/record/display.uri?eid=2-s2.0-0028856859&origin=inward&featureToggles=FEATURE_NEW_DOC_DETAILS_EXPORT:1#metrics Subscription required.

14. Daewa R, Saneha P, Bhuthathorn L, Thetasen N. Spontaneous regression of the lung bulla. ASEAN J Radiol [Internet] 2021 [cited 2022 Jan 16]; 22(3) : 41-6. Available from: https://www.asean-journal-radiology.org/index.php/ajr/article/download/154/107/1534

ASEAN Movement in Radiology

Many good reasons to attend "The 21st Asian Oceanian Congress of Radiology (AOCR)" in Bangkok, Thailand

Wiwatana Tanomkiat, M.D.[(1)]
Jarturon Tantivatana, M.D.[(2)]
Theerapol Panyaping, M.D.[(1)]
Napapong Pongnapang, Ph.D[(2)]
Alongkorn Kiatdilokrat, M.D.[(1)(2)]
Dittapong Songsaeng, M.D.[(1)]
Pittaya Dankulchai, M.D.[(2)]
From [(1)]The Royal College of Radiologists of Thailand
[(2)]Radiological Society of Thailand
9th floor, Chalermprabarami 50th Anniversary Building, Soi Soonvijai,
New Petchburi Road, Bangkok, Thailand.
Address correspondence to W.T. (e-mail: twiwadha@hotmail.com)

Received 25 August 2022 ; accepted 25 August 2022
doi:10.46475/aseanjr.v23i2.183

Keywords: 21st Asian Oceania Congress of Radiology, AOCR, 2023.

THE ASEAN JOURNAL OF RADIOLOGY
ISSN 2672-9393

Congress Title:
The 21st AOCR and 59th RST-RCRT Congress

Congress Theme:
Redefining the possibilities in medical imaging

Date: 9-12 February 2023

Congress Venue: Centara Grand & Bangkok Convention Centre at CentralWorld

Website: www.aocr2023.com

Email: secretariat@aocr2023.com

Hosts:
The Radiological Society of Thailand (RST)/
The Royal College of Radiologists of Thailand (RCRT)

Remark:
2023 will celebrate the 60th anniversary of RST

Why Thailand:
- Strategic location in Southeast Asia
- 1st Asian holiday destination 2021
- 5th conference destination in Asia 2019
- Top 5 countries in the world with " The hospitable host DNA"
- Thai Visa is exempted for 64 countries while the other 18 countries can apply for "Visa on Arrival"
- Easy and safe to get around the country as shops, restaurants, and convenient stores are mostly open 24/7
- Tourist service center can be found in many places of attractions throughout the country
- Hotline 1155 for any enquiries related to foreign visitors to Thailand
- Thailand's response to the COVID-19 pandemic revealed the strength of its healthcare capacity

Why Bangkok:
- A bustling metropolis that truly represents Thai uniqueness
- Most Visited City in the world
- A gateway to the Kingdom of Thailand
- A knowledge hub of the country
- UNESCO Creative City of Design
- Ranked 13th among healthiest cities worldwide
- Smart city development amidst rich Thai culture and its age-old charm
- An important aviation hub with 2 international airports served by over 80 airlines linking 170 cities worldwide
- Only takes 40 minutes from the airport to downtown by car with the 35 USD airport limo rate or 10 USD taxi rate
- It is convenient and safe getting around Bangkok by BTS sky train and MRT underground. There is also a major bus network crisscrossing the city. Grab Taxi is also a popular option nowadays in metropolis area.

Organizing Chairman:
Asssistant Professor Jarturon Tantivatana, M.D.
President, The Radiological Society of Thailand

Welcome Message:

Dear colleagues,

On behalf of the Organizing Committee, we are pleased to invite you to the 21st Asian Oceanian Congress of Radiology (AOCR 2023) which will be held in conjunction with the 59th Annual Scientific Meeting of the Royal College of Radiologists of Thailand and the Radiological Society of Thailand, in Bangkok, Thailand.

The AOCR 2023 will be held at the Centara Grand and Bangkok Convention Center from February 9-12, 2023 under the theme "Redefining the Possibilities in Medical Imaging". The venue is sitting in the heart of Bangkok with astounding surroundings, full facilities, convenient traveling and cozy accommodation.

Participants will have good chances to participate in on-site events again after a few years of pandemic restrictions and meet other international colleagues face to face in warm Thai hospitality. There will be many interesting radiology scientific sessions including diagnostic imaging, interventional radiology, application of artificial intelligence, radiation safety and evolving practice standards.

We look forward to welcoming you and appreciate your participation in the AOCR 2023.

Best wishes and see you in Bangkok.

Scientific Chairman:
Associated Professor Wiwatana Tanomkiat, M.D.
President, The Royal College of Radiologists of Thailand

Welcome Message:

It is time to redefine the possibilities of medical imaging!

Challenges and opportunities are inevitably embedded to a crisis depending on which perspective we look at. During a couple of years of drowning in the COVID-19 pandemic, some existing concepts, means, work flows and tools failed to respond timely and effectively. Governments, industries, private sectors, and non-profit organizations have exerted all their efforts and resources to sustain the citizens' livelihood by ensuring the smallest rate of morbidities and mortalities of the people to their full potential. New products and innovations were introduced and accepted at an unprecedented speed. Apparently, imaging, and related informative technological systems, serving as an important part in health industries, plays an indispensable role in triaging, diagnosing and caring for the COVID-19 patients.

While the COVID-19 pandemic is still on-going, new knowledge and experiences are increasingly obtained. It is time to talk and share on the issue. The 21st AOCR in Bangkok, Thailand will provide the best opportunity in a friendly atmosphere for scientists, technologists and radiologists to share what they have acquired, what we should adopt and how we can adapt to improve our facilities in caring not only for COVID-19 patients but also patients inflicted with other diseases that threaten the health of people and burden the countries in Asia-Oceania.

THE ASEAN JOURNAL OF RADIOLOGY
ISSN 2672-9393

Bangkok, the charming capital of Thailand, always hospitably invites people from around the world to experience the unique culture, world-class cuisine, and heartfelt hospitality in her almost 250-year-old history. Her beauty is at the peak in February when the weather is kind and the sun is warm. On behalf of the scientific committee, I encourage new technologies to be exhibited, new knowledge to be presented, and new relationships to be formed during 9-12 February 2023 in the 21st AOCR, Bangkok, Thailand. Again, I am certain that the 21st AOCR will provide the best time and place to redefine the possibilities of medical imaging in the future.


Scientific Committee:
Assistant Professor Theerapol Panyaping, M.D.
Assistant Professor Napapong Pongnapang, Ph.D

Trade and Exhibition:
Alongkorn Kiatdilokrat, M.D.

Social Program:
Associate Professor Dittapong Songsaeng, M.D.
Associate Professor Pittaya Dankulchai, M.D.

Supportive organizations:

- Nuclear Medicine Society of Thailand
- The Thai Medical Physicist Society
- The Thai Society of Radiological Technologists
- The Thai Society of Vascular and Interventional Radiology
- Thailand Convention and Exhibition Bureau
- Thailand Incentive and Convention Association
- Thai Hotels Association

ASEAN

This journal provide 4 areas of editorial services: language editing, statistical editing, content editing, and complete reference-citation check in 8 steps:

Step	Services to authors	Services providers
I	Manuscript submitted	Editor
II	Language editing/ A reference-citation check	Language consultant/Bibliographer
III	First revision to ensure that all information remains correct after language editing	Editor
IV	Statistical editing	Statistical consultant
V	Content editing*	Two reviewers
VI	Second revision	Editor
VII	Manuscript accepted/ rejected	Editor/Editorial board
VIII	Manuscript published	Editorial office

*Content editing follows a double-blind reviewing procedure

JOURNAL OF RADIOLOGY